Design, Development and Characterization of a Wrap Spring Clutch/Brake Mechanism as a Knee Joint for a Hybrid Exoskeleton

by

Vishnu Aishwaryan Subra Mani

A Thesis

Submitted to the Faculty

of the

WORCESTER POLYTECHNIC INSTITUTE

In partial fulfillment of the requirements for the

Degree of Master of Science

in

Mechanical Engineering

May 16, 2020

APPROVED:

_____

Professor Gregory S. Fischer, Thesis Advisor

_____

Professor Zhi Li, Committee Member

_____

Professor Cagdas D. Onal, Committee Member

_____

Professor Pratap M. Rao, Graduate Committee Representative

Abstract

Evolution had played a significant role in structuring on how humans stand, walk or run. The nervous system plays a major role in the control of locomotion and injuries to the system can lead to gait abnormalities or disabilities. A Spinal Cord Injury (SCI) causes lack of signal communication between the central nervous system and the muscle fibers leading to deprived or no activation of the muscles thus resulting in paraplegia or quadriplegia.

Over the past decade wearable robotics and exoskeletons have been gaining outstanding recognition in the field of medical, assistive and augmentative robotics and have led to numerous new innovative mechanisms in the mechanical engineering field. Due to fast paced research activities, the critical importance and performance of mechanisms such as wrap spring clutch/brake,Wafer Disc brakes are overlooked or used ineffectively. So, researchers tend to create new actuators from scratch and have limited their use of previously available resources, which has prevented us to explore the potential of these devices.The research presented focuses on developing a mechanism ("A Wrap Spring Clutch/Brake Mechanism") from scratch using a trade study approach. This thesis addresses the fundamental relationship between coefficient of friction, interference, spring diameter and the holding torque of the mechanism using analytical, testing and simulation results. The human biomechanical data during ground level walking was used as design targets to develop the mathematical model of the system. Data from the testing stated that these targeted goals have been achieved by the design. This mechanism is used as a Knee Joint for the Hybrid EXoskeleton (HEX) GEN-1 project which is developed at the Automation and Interventional Medicine (AIM) Robotics Research Laboratory to rehabilitate the SCI.

Acknowledgements

The working of HEX GEN-1 is due to the inputs and support from many people. Firstly, I would like to express my gratitude to Adnan Munawar, Radian A Gondokaryono, Christopher J. Nycz and all my lab members for their suggestions and thoughts during the design process. I would like to thank my team members Andrew Nagal, Nathaniel I. Michaels and Benjamin J. Secino for their coordination during the design and trials. Thank you, Mr. Ian Anderson, Mr. James Loiselle and Matthew Dick for you support and guidance during manufacturing. I am deeply grateful to my mentors Nathaniel Goldfarb and Michael A. Conrad for their constant support and their assistance during programming and electrical wiring of the HEX.

I am greatly thankful to my committee members Prof. Zhi Li, Prof. Cagdas D. Onal and Prof. Pratap M. Rao for their constant support throughout the process. Prof. Onal and Prof. Li, thank you for letting me to audit your Soft Robotics and Human Robot Interaction courses. These topics gave me a new perspective on designing an exoskeleton and some novel ideas to incorporate in my future work. Prof. Rao, the time that I have worked with you during the course and now you have been supportive, and your feedback was really helpful during writing and to maintain my timeline.

Finally, I would like to convey my heartfelt thanks to Prof. Gregory S. Fischer for advising me and for helping me take my very first step in the field of exoskeleton and for bringing my dream to reality. Your motivation and your love for medical devices gave me an opportunity to work and learn about rehabilitation robots and the way it can improve the people's life. Moving forward in my career I will apply all the things that I have learnt from you in making this world a better place for people with disabilities.

Dedication

To all the researchers across the world who are passionate about making a difference in this world - you have inspired me into the research field.

To all the Spinal Cord Injured people - your determination is my motivation.

And to my mom and dad, thank you for dedicating your life's work for supporting me and for giving me this opportunity. Mom, your passion for medicine and my childhood memories in your college motivated me to take a career in this domain. Dad thank you for teaching me the lessons about life.

Contents

List of Figures

List of Tables

0.1 List of Acronyms

SCI Spinal Cord Injured

FES Functional Electrical Stimulation

HEX GEN - 1 Hybrid EXoskeleton GENeration - 1

MR MagnetoRheological

ER ElectroRheological

NC Normally Closed

FSR Force Sensitive Resistor

IMU Inertial Measurement Unit

EMG ElectroMyoGraphy

CAD Computer Aided Design

CAM Computer Aided Manufacturing

LIDAR Light Detection and Ranging

PLA PolyLactic Acid

CNC Computer Numerical Control

FEA Finite Element Analysis

DOF Degree of Freedom

Chapter 1

Introduction

1.1 Motivation

Over the past decade exoskeletons have assisted, rehabilitated and augmented human movements like walking, running and lifting weights. Companies, startups and research labs are focused on promoting the advantages of exoskeletons among the common population [32],[7],[2] . Exoskeletons are used for both upper and lower body rehabilitation, but in this current project we will be focusing mostly on lower body rehabilitation. The use of exoskeletons to restore gait activities for SCI have been commonly observed in a lot of rehabilitation centers around the world.

During the early stages of exoskeleton development, orthotics played a crucial role. The initial years of research for restoring legged mobility in paraplegics included passive orthotics, systems like Hip-Knee-Ankle-Foot-Orthoses (HKAFO), Hip Guidance Orthosis (HGO), Stance-Control-Knee-Ankle-Foot-Orthoses (SCKAFO) which were constrained at the hip, knee, and ankle joint along the sagittal plane to assist movement. But these constraints have shown significant increase in metabolic energy costs due to higher level of physical exertion. [17][13][1].

Due to recent advancements in electro-mechanical and sensor technology, researchers are exploring ways to study the mechanics behind human movement. Sensors like EMG, Motion Capture, IMU, help track the joint movements and muscle activities during gait instances which reveal the firing order of muscles.

Based on dynamic and kinematic model, actuators were used in orthoses, to emulate human like walking. Several trials [36], [23] have shown that users metabolic cost have reduced due to the use of assistive device.

This technology in the past few years have led the non ambulatory population to walk again and have shown technological advancements in the field of robotics.

1.2 Biomechanics

1.2.1 Muscles and Planes

A human body can be transected in three ways:

Left and Right - a sagittal (longitudinal, anteroposterior) plane divides the body into two identical mirrored parts

Dorsal and Ventral - a coronal (vertical) plane divides the body into back(posterior) and front(anterior)

Cranial and Caudal - a traverse (lateral, horizontal) plane divides the body into upper and lower extremity

Most exoskeletons assume that the human gait is constrained along the sagittal plane. Another common assumption is that the joints (hip, knee and ankle) are modelled as a pin/hinge joint. Each joint along this plane has a direction of flexion and extension which is controlled by a set of agonistic and antagonistic muscles which control human walking. The maximum range of motion of the joints in the sagittal plane is represented in fig.1.1

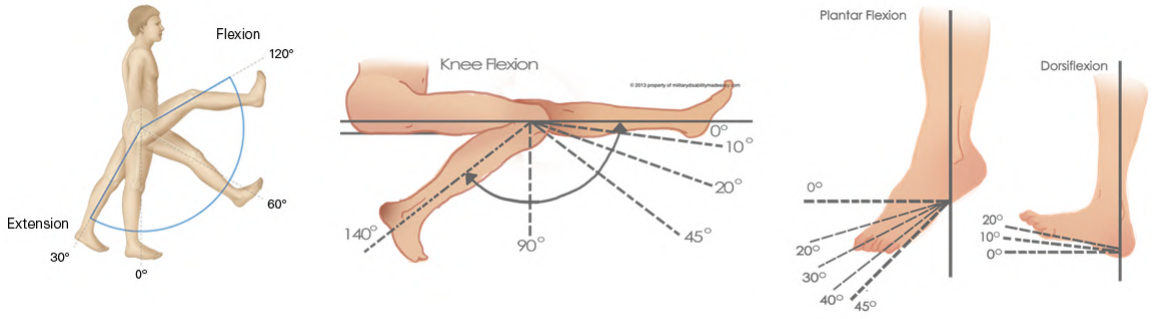

Figure 1.1: Direction of Flexion/Extension of Hip, Knee and Ankle [31] [30] [21]

There are almost 640 skeletal muscles in the human body and the mind map represented in fig 1.2.1 lists the names of the muscles in a leg.

In this wide list, a major set of muscles play a crucial role in the control of human walking. This set of muscles is listed in table 1.1 and is shown in fig. 1.3

Muscle	**Controlling Joint**	**Gait Instances**
Gluteus Maximus and Tibialis anterior	Hip and Ankle	Heel Strike
Quadriceps Femoris and Triceps Surae	Knee and Ankle	Loading Response
Triceps Surae	Ankle	Midstance
Triceps Surae	Ankle	Terminal stance
Rectus Femoris	Knee	Preswing
Iliopsoas and Rectus Femoris	Hip and Knee	Initial and Mid Swing
Hamstrings, Quadriceps Femoris and Tibilais anterior	Knee and Ankle	Terminal Swing

Table 1.1: Muscles Controlling Walking

Figure 1.2: Mind Map of Lower Body Skeletal Muscles [24]

The muscles that are activated during the stages of gait is listed in figure 1.3

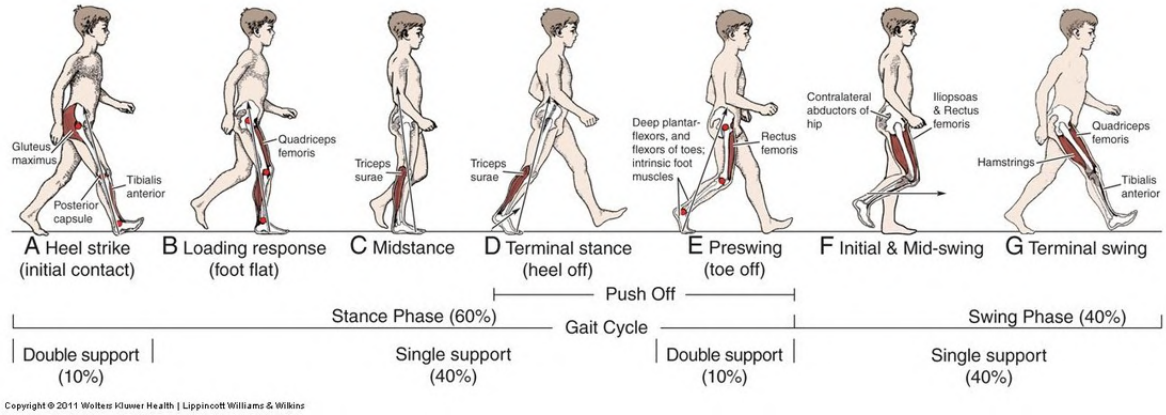

Figure 1.3: Group of Skeletal Muscles Activation during gait [27]

1.2.2 Gait Joint Characters

From fig 1.3, fig 1.4 we can conclude that positive power is produced at the hip during heel strike and preswing phases and at the ankle during the terminal phase of the gait. During the gait, the knee dissipates most of the energy. Negative power is observed at the ankle during midstance and at the hip during terminal stance to support the body and to hold the body against the gravity when propelled forward.

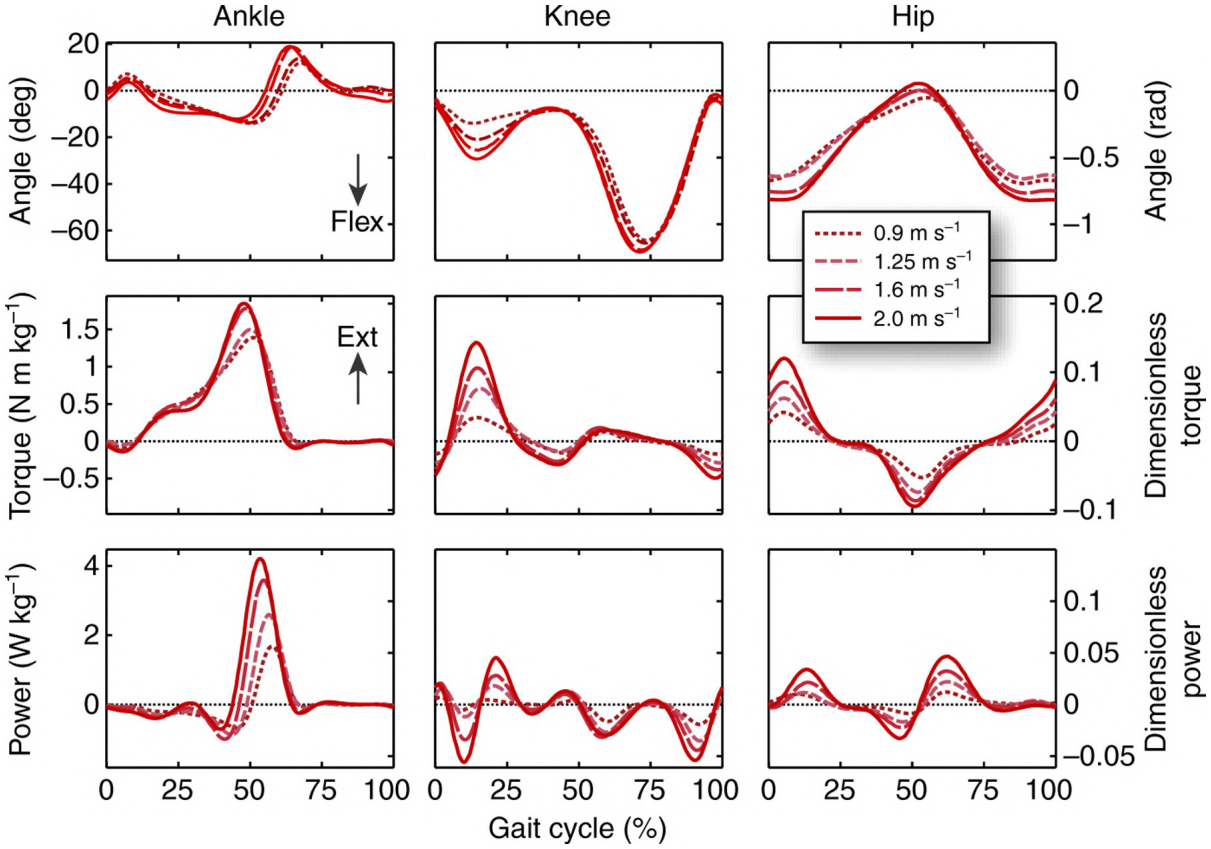

Figure 1.4: Joint Angles [38]

Throughout literature it has been mentioned that in a power plot of a joint, if a negative power precedes a positive power it can be modelled as a spring joint. In the gait cycle this can be observed at the hip joint during the transition from terminal stance to preswing and at the ankle during the transition from midstance to preswing and at knee during early stance to midstance.

[34] and [25] have talked extensively about the sit to stand transition and have plotted graphs representing the moment, angle and power generated at the joints during this process. In this study the author assumed the seated knee angle to be zero degree and as the user transitions from sit to stand posture the angle increases.

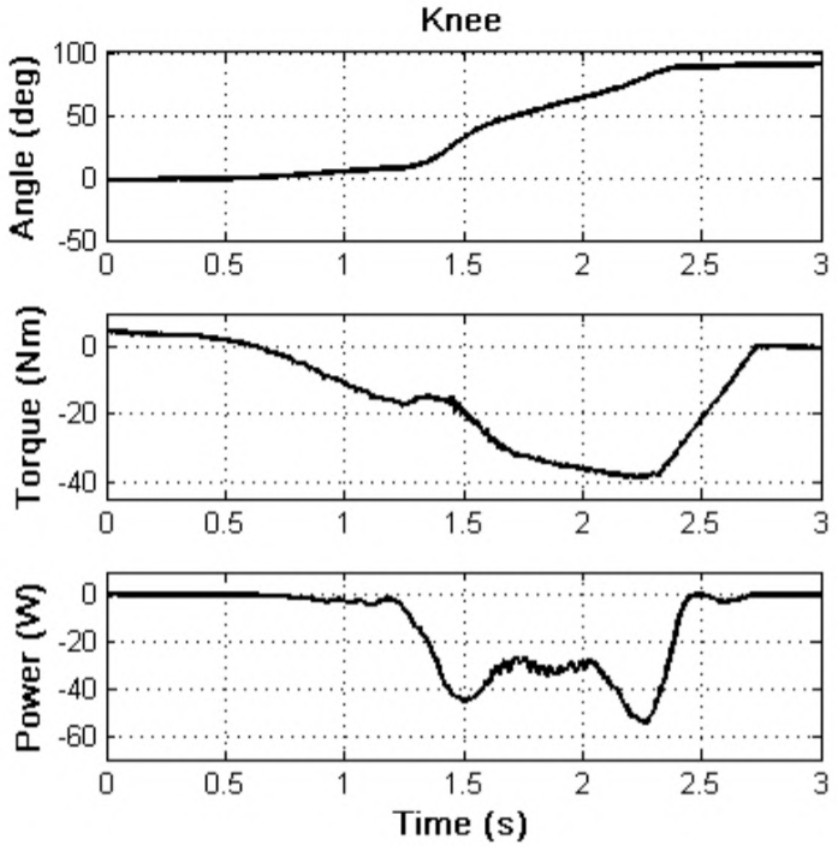

Figure 1.5: Sit to Stand Knee Joint Behavior [34]

From plots we can observe that the power in the joint increases during the initial phase of the transition and as the knee extends to a straight posture the power produced by the knee falls back zero. The zero power value at midstance of the gait and the standing posture states that the muscles are not active during these phases. Hence in order to preserve the movement the knee joint is locked and the wight is transmitted to the ground.

1.3 Thesis Contributions

The motivation towards this work is to study existing systems to estimate a potential device for he HEX GEN-1's walking activity. The performance of mechanical devices have saturated over the years due to fast paced research activities and lack of continuous development of existing technologies.

The research presented here focuses on this issue by developing, testing and understanding the fundamentals of an actuator based on the requirements of human walking.

Contribution 1

Biomechanical data such as range of motion, torque and power during an activity can be studied using motion capture system and can be set as a design targets.

Question 1 If such an actuator satisfying the target exists, then what parameters control the holding torque of the system and how can a system be designed to be weight efficient?

Contribution 2

This project will explain the reasons behind the design, simulation and testing of the actuator which can lead to development of new cheaper systems which can be affordable.

Question 2 After understanding the basic model of the actuator are there any new design solutions to improve the holding torque capability? If so, what are the parameters that have to be changed?

1.4 Thesis Outline

The background work carried out by companies and researchers are shown in **Chapter 2**.

Chapter 3 explains the human trials, trade study and mathematical model of the design.

A detailed step by step process behind the hardware design and the testbed is explained in **Chapter 4**. It also provides information about the manufacturing process and some important techniques that can be used to fabricate the parts.

Chapter 5 explains the testing techniques and the reasons for testing. An overview of the test bed and the procedure is documented for future reference.

Chapter 6 specifies the optimization technique used for simulations and the steps behind the process.

The results of testing, analysis and human trials are included in **Chapter 7**. By the end of this step we have studied the model and understood about the function of the system properly.

Chapter 8 includes conclusion, future work and design changes to improve the function of the system.

Appendix A includes drawings for all parts.

Chapter 2

Literature

2.1 Background

The HEX GEN-1 was developed at the WPI AIM Lab to rehabilitate SCI using a hybrid approach. It combines the advantages of FES and actuators to improve muscle and bone density of the user. The mechanical design of the HEX, inputs work from the following authors, Andrew Nagal on the hip joint, Vishnu Aishwaryan Subra Mani on the knee, Nathaniel I. Michaels on the ankle joint, Nathaniel Goldfarb's doctoral research inputs and Michael Conrad's work on the control board. The frame for the design was made out of Aluminum 6061. The back plates and the side rails on the hip can be adjusted to fit individual's hip width and joint axis, the links connecting the joints are made using concentric hollow tubes and rods, which can be changed based on the user's height.

For the purpose of our current design, the hip, knee and ankle are treated as a pin joints along the sagittal plane. The Hip joint uses a EC 90 Maxon Motor and a harmonic drive to assist hip flexion/extension. The knee is designed as a quasi-passive brake whose details are explained in the later sections. The ankle uses a Dorsiflexion restoring spring to avoid foot drop and to bring the foot to its neutral position after the toe off phase in

the gait cycle.

The system uses data from multiple sensors to sense the robot's current state. There are 7 IMUs one at each joint and one mounted to the control board which is located at the back. The knee and ankle joints have a potentiometer to gather joint angle data and the hip motor has an inbuilt encoder to measure joint angles at the hip. The footpad uses 3 FSRs to detect heel strike and toe off during the gait which is used to estimate the exoskeleton's foot touchdown during the the gait. Currently LIDARs are mounted on the hip to map the surrounding to gather data for obstacle avoidance and for path planning.

Apart from these sensors, during trials Vicon motion capture system and EMGs were used to sense and validate the gathered data.

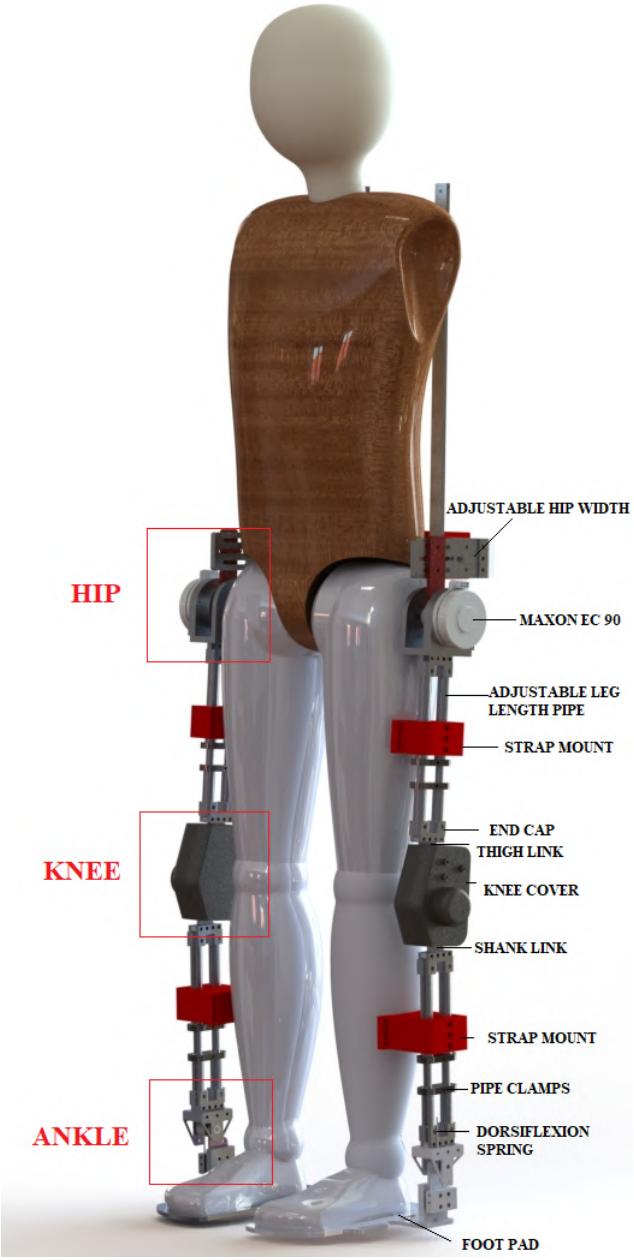

Figure 2.1: Rendered Image of the HEX

A lot of requirements for the design were developed based on literature and human trials.

2.2 Previous Work on Orthoses

Researchers around the world [9],[17],[3],[4],[2], [20], [37] are in the process of developing lower extremity exoskeleton for different applications and at cheaper prices.

(a) Ekso Bionics (b) Rewalk (c) HAL

Figure 2.2: Market Available Exoskeletons

Exoskeletons developed in research laboratories like the Austin Exoskeleton from UC Berkeley and powered exoskeleton from Vanderbilt have provided access to information about the type of actuators. Tung [33] mentions about a Parker BE231D Brushless DC motor used in the hip joint to provide 53Nm of continuous and 160Nm of intermittent torque. The behavior of the knee joint is controlled using an off the shelf one way locking gas spring.

The following images represents the actuators used in the Austin Exoskeleton.

(a) Austin Exoskeleton [33]

(b) Austin Hip Joint [33]

Figure 2.3: Berkeley Exoskeleton

[33] uses a wrap spring clutch design at the knee to assist the user during level ground walking while the next generation mentioned in [26] uses a dual joint wrap spring clutch gas spring knee where the braking cycle was executed using wrap spring clutch and the powering cycle was produced by the torque generators (Gas Spring) to provide additional thrust to propel the body during other activities such as stair climbing. The images of

the knee joints are represented in fig 2.6a and 2.6b,

The wrap spring brake's quasi-passive nature allows it to hold high torque values. In [19] and [33] the mechanism is explained by the movement of the arbors, where two concentric arbors and a spring are assembled as represented in figure 2.4.

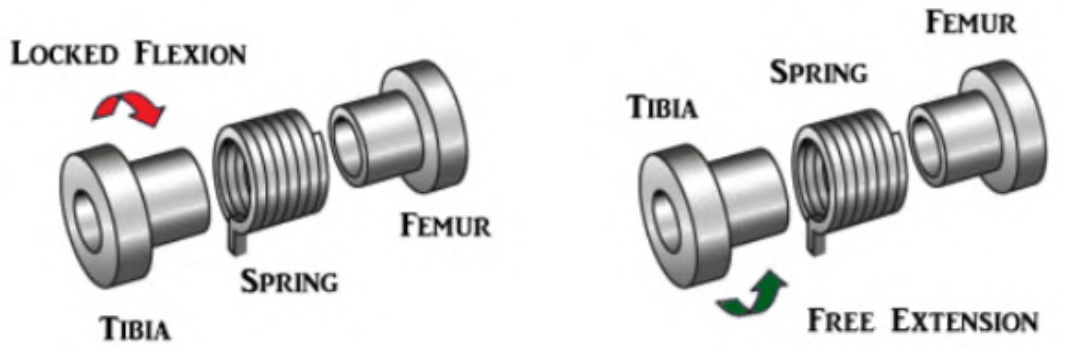

Figure 2.4: Mechanism behind wrap spring clutch [19]

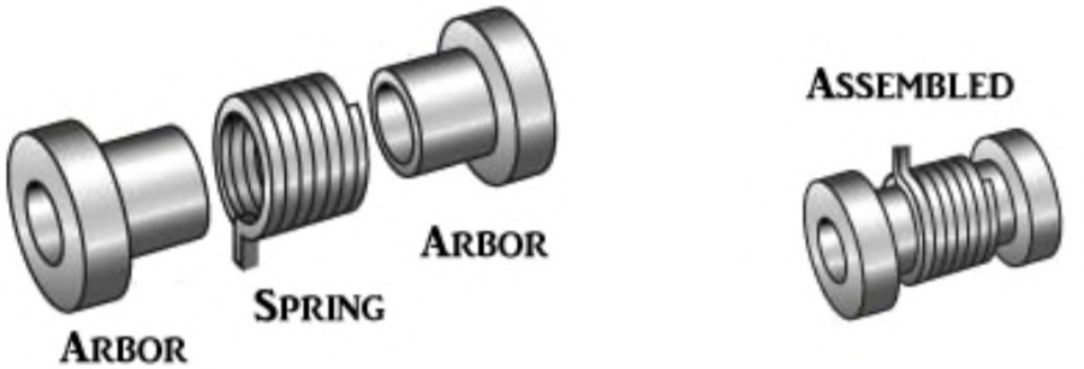

Figure 2.5: Assembly of Simple Wrap Spring clutch [19]

Fig.2.5 shows an exploded and an assembled view of a simple mechanism. In this setup the diameter of the arbor is slightly greater than the inner diameter of the torsion spring which causes an interference. So, when assembled there exists an initial contact pressure between the arbor and spring. When this mechanism is integrated as the knee joint, one arbor is connected to the femur and the other to the tibia where the latter is the rotating component. So, during knee extension the relative motion between the

arbors allows free movement between the joint and during knee flexion the relative motion causes the wrapping effect.

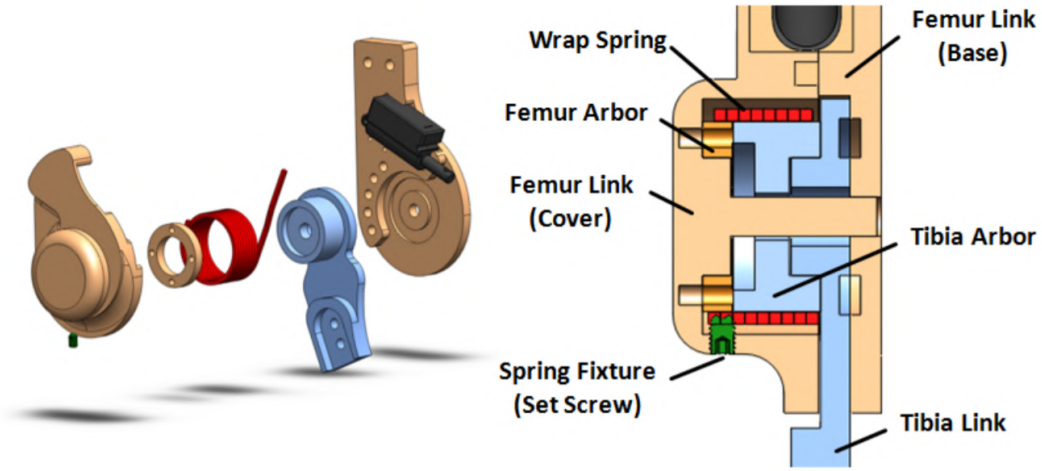

(a) Wrap Spring Clutch/Brake Knee by Tung [33]

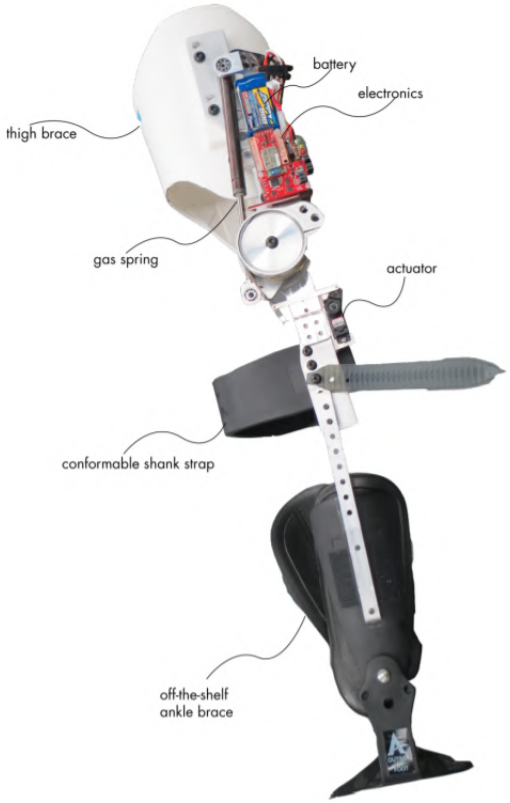

(b) Dual Joint Knee by Pillai [26]

Figure 2.6: Knee Joints of Austin Exoskeleton

The exoskeleton mentioned in [16] is a hybrid device which uses FES with a mo-

tor/brake system to assist SCI patients during walking. This approach has shown improvement in muscle mass and bone density of the user. When a traditional FES system is used, multiple muscles are activated to hold the user in an upright posture. But by incorporating a hybrid approach, the joint locking can be executed using a mechanical system which will increase the cycle of muscle activation during the rehabilitation session. Results from the trials have shown improved performance with the device on.

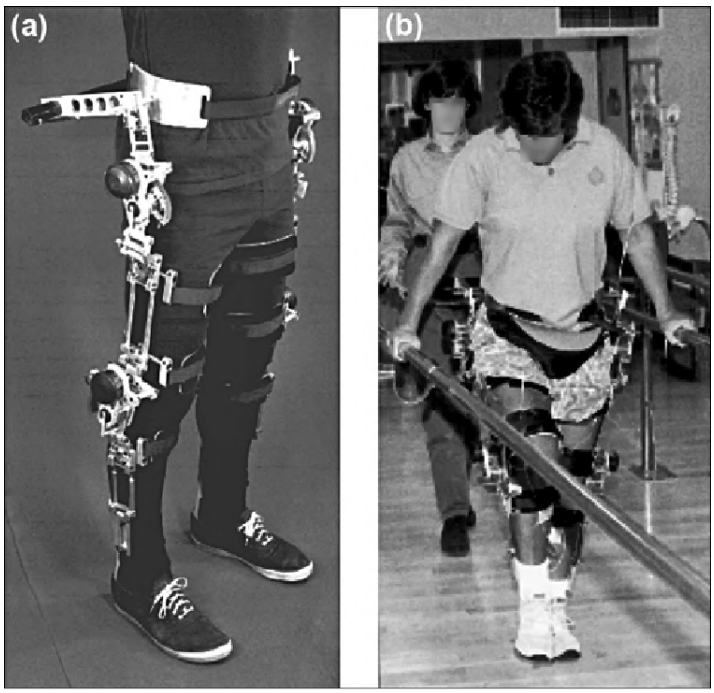

Figure 2.7: Hybrid FES Exoskeleton [16]

[23], [35] integrates actuators, brakes and gearing mechanism using MR or ER fluids at the knee joint to assist elderly and disabled people. These devices provide additional torque at the joint to overcome mobility issues during stair climbing and to cross large obstacles during walking.

In [15] a magnetic particle brake is integrated in a Controlled Brake Orthosis has shown reduction in muscle fatigue during repeated loading when compared to traditional FES gait systems.

In [14] the author mentions that surface stimulation is hard to achieve at the hip joint due to large amount of muscle and skin interference. Due to this issue they built a hybrid FES Joint Coupled Controlled Brake Orthosis system to provide hip flexion and to propel the leg in the forward direction. They have used a new type of hip and knee brake which is called as Wafer Disc Brakes. The system integrates normally closed type brake which remains engaged even during times of power failure thus enabling wearer's safety. The other key aspect mentioned is the longer walking time which is achieved by intermittent braking at the joints.

The brake utilizes a series of stacked high strength wafers/discs where the stator and rotor components are placed alternatively with a small distance. A small motor is connected to the center shaft and when this motor is engaged a compressive force is given via the ball screw to the discs. Thus, this compressive force between the stator and the rotor discs causes the system to brake which is a determined by the amount of current given. The parameters that decide the braking capability are the friction coefficient of the discs, area of contact and the contact pressure. To achieve higher holding torque capability, they have increased the surface area of contact by increasing the number of discs. The hip joint braking system consists of 61 discs and 60 discs are at the Knee joint thus producing effective braking. Figure 2.8a illustrates the system and the cross-sectional representation of the brake.

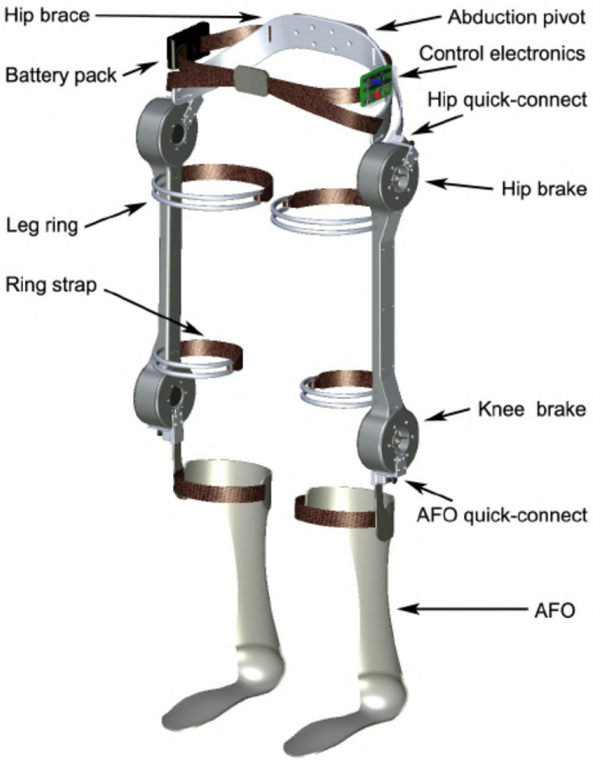

(a) Joint Coupled Controlled Brake Orthosis

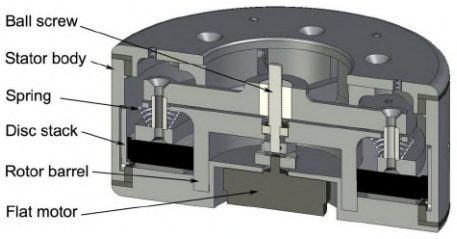

(b) Cross Sectional View of Wafer Disc Brake

Figure 2.8: Hybrid FES JCO Exoskeleton [14]

[5] has developed a Variable Impedance Knee Mechanism to provide assistance for people with weakened knee extension. The mechanism used in the knee joint uses a linear MR fluid damper and four bar linkage mechanism to provide eccentric quadriceps like contraction. This controls the level of knee flexion at different stages of stance phase of the gait and during stair descent. A maximum torque of 64.5 Nm is produced by the system with a very less passive resistance of 4Nm at 210^o/s. The entire orthosis along with the damper, links and AFO weighs around 3.5 Kg. The schematic diagram of the concept and the orthotic device is represented in the fig 2.9.

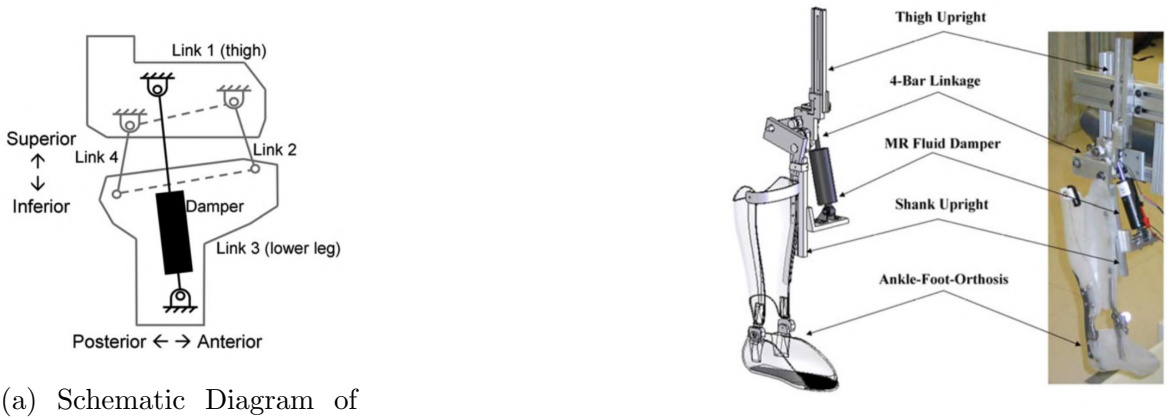

(a) Schematic Diagram of Variable Impedance Knee Mechanism

(b) Variable Impedance Knee Mechanism

Figure 2.9: Variable Impedance Knee Mechanism Orthosis [5]

The knee joint mentioned in [28] represents a knee exoskeleton which functions using a series elastic actuator which acts based on the controller's use. An off the shelf knee brace is integrated with this actuator and is mounted around a healthy human which integrates load cells in the shoes. Thus, the entire mechanism was controlled based on the user's intent to move and the mechanism enhances users movement and provides enough energy to counteract the work done against the gravity. The exoskeleton weighs 2.5lbs and can provide a continuous force of 127 lbs. Fig 2.10 gives a representation of the exoskeleton along with the name of the parts.

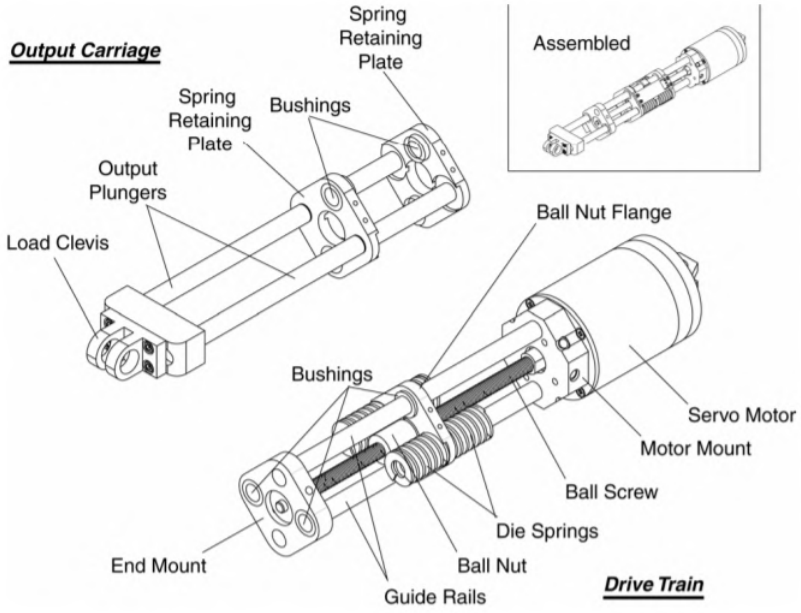

Figure 2.10: Series Elastic Actuator of RobotKnee [28]

The vanderbilt powered orthosis mentioned in [13] integrates brushless dc motors with a 24:1 gear box at the hip and knee joints which provides a maximum assistive torque of 40 Nm. The orthosis weighs 12kg in total. At the knee joint a brake is integrated along with the motors system. Features about the range of motion of the joints, profile of the orthosis on the frontal plane and the user's ability to sit in an armchair or wheelchair were considered carefully during the design of the orthosis which is shown in fig 2.11

Figure 2.11: Vanderbilt Orthosis [13]

The Clutch Spring Knee designed for running has a compact high-performance design. In [11] a parallel elastic exoskeleton is built to replicate the spring like behavior of human leg during running gait. It uses a clutch mechanism to disengage the leaf spring during the swing/aerial phase of the running gait and engages the clutch during the stance phase. The clutch uses a planetary gear transmission which is coupled to a rotating clutch plate. The engagement and disengagement of the clutch is enabled using a solenoid and a sliding clutch plate. This setup has an ability to withstand high holding torque due to the number of teeth in the clutch plate which are made of titanium alloys of grade 2 and 5. This reduced the weight of the system to 710g and has a holding torque capacity of 190 Nm. The biomechanical study shows that the human knee experiences a torque of about 150 Nm during running. So, they designed the joint using safety limitation values and when the solenoid engages the clutch and locks the knee joint at the end of swing phase/pre-contact phase the bow like leaf springs are loaded thus storing energy during this phase. During the Terminal stance phase the clutch disengages and

allows free swing motion.

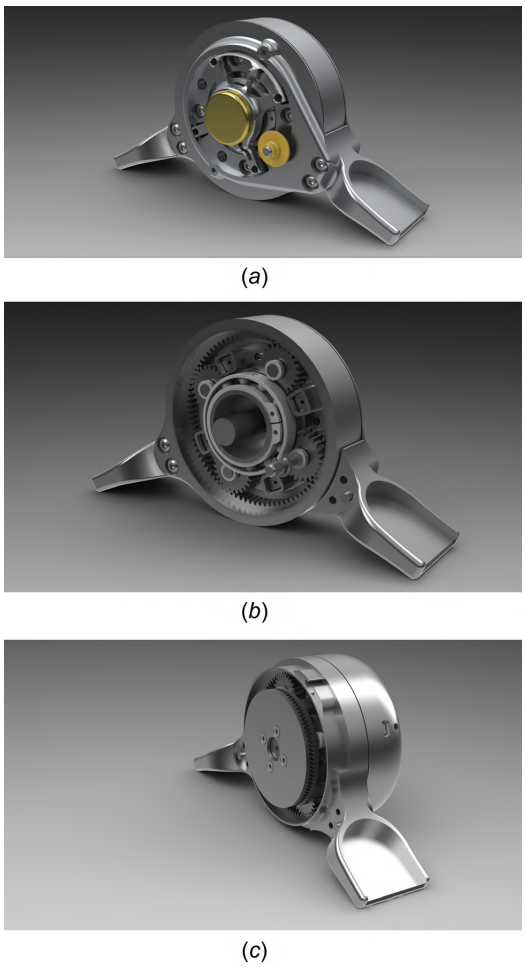

Figure 2.12: Clutch Spring Knee Exoskeleton for Running [11]

In [22] the author uses a market available prosthetic knee (Rheo Knee by Ossur Inc) to study the relationship between braking torque and magnetic field strength. Based on this relationship the author executed new design changes to the device to achieve maximum performance. The device uses a MR brake at the knee and the resistance in the flexion direction is controlled by the strength of magnetic field applied to the MR fluid. The brake consists of a stator and rotor which consists of steel plates which are stacked alternatively. The center of the system includes a Ferrous- Cobalt core which when energized results in magnetic field. The outer and inner surfaces are covered

with non-ferromagnetic material like titanium and aluminum. The stator and rotor are coupled to the residual limb and shank link respectively. Thus, when a magnetic field is applied a shear force causes the disc/steel plates to come to rest and arrests the motion. The mathematical design behind the mechanism is explained in detail. A final conclusion states that increasing the radius of the actuator or increasing the number of steel plates has a major impact on the holding/braking torque value.

This figure shows the cross section of the MR Brake

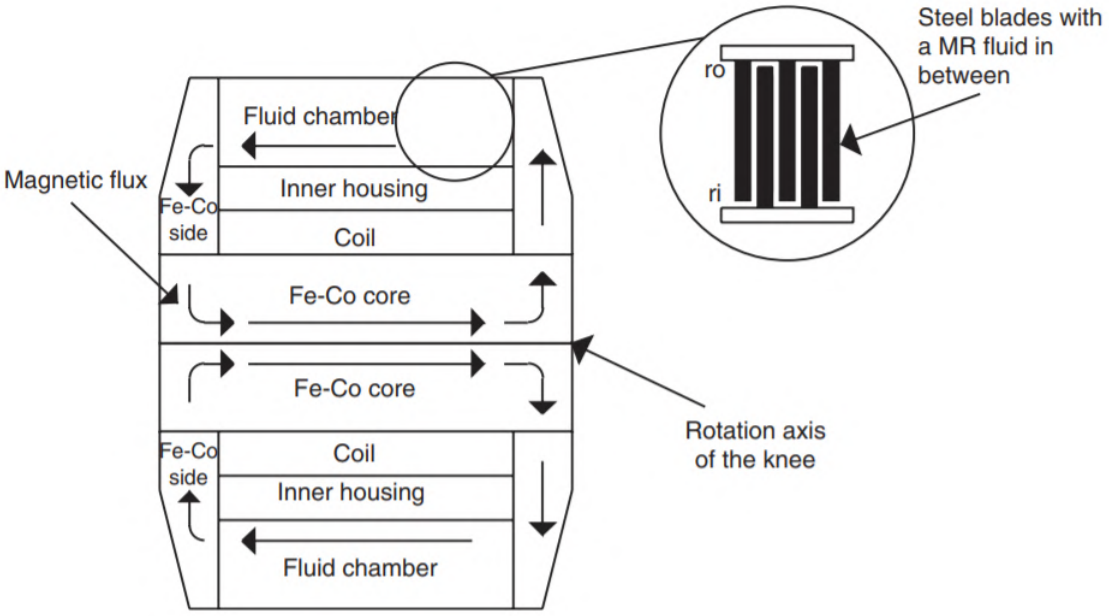

Figure 2.13: Cross Section of MR Brake in Rheo Knee [22]

Currently there are a number of actuator designs available to various research groups. But the quality and testing aspects such as lifecycle, cost, durability and performance on testing or human subjects are not mentioned. The lack of knowledge on these details have stagnated improvements in these devices. Thus based on our application and requirement we used a trade study to select a device and we studied the system from scratch to utilize the system to its utmost potential.

Chapter 3

Design and Analytical Approach

3.1 Trade Study

The following are the functions based on which the existing systems were weighed and the reasons for choosing these functions are well elaborated as well.

3.1.1 Weights for Study

This trade study reviews different mechanisms to select the best knee for the desired requirements. We found some common features in a certain number of papers that the designers tend to consider. The criteria mainly include cost/manufacturing, mass, power requirements, lifetime/serviceability, safety, holding torque, miscellaneous. Our weights for the criteria are based on the frequency of its appearance across several papers.

To further improve their design, the designer can add any new design criteria and change the weights accordingly. Then these criteria can be evaluated across existing or new mechanical systems to find the best-suited mechanism for the chosen application. The total value of the weights must account to 100, representing the efficiency of the design.

By following processes such as this, we can develop preliminary standards to improve the quality of exoskeletons. The criteria and weights for the HEX GEN-1 knee are listed as follows.

- **Manufacturing Cost and Simplicity (10)**

  The existing exoskeletons in the market cost thousands of dollars, which makes them inaccessible. There is a need to make exoskeletons more affordable [10], [18]. This work motivated us to make our exoskeleton affordable. Hence we leaned towards common inexpensive materials such as steel and aluminum. We assigned this criterion a weight of 10.

- **Mechanism Mass (15)**

  The mass of the system is a significant design criterion in many wearable devices [29]. The mass of the actuators in the literature varied over a wide range, starting from $0.3Kg$ to $3.5Kg$ for the same holding torque. To achieve a lightweight system, we chose an upper bound weight value of $1.5Kg$ for a knee joint. This mass range is standard in prosthetic devices. The nominal weights for a prosthesis are characterized based on body segment weight, which lies within this limit too. We assigned this criterion a weight of 15.

- **Power requirements for actuation (10)**

  We built the current version of HEX GEN-1 to execute ground-level walking. Biomechanical data and literature mentioned that this could be achieved using quasi - passive devices. Intuitively we could say that such a selection can make the exoskeleton work for a longer duration. This aspect motivated us to look for quasi-passive mechanisms. We assigned this criterion a weight of 10.

- **Lifetime and Serviceability (12.5)**

  The lifetime of the device is a critical factor for machine elements, and it has to last

for repeated cycles without breaking. The lifecycle of the exoskeleton mechanisms has not been widely reported. We considered that by including this criterion in this study, the potential of specific overlooked devices in the research field could be addressed. This quantity can be used to track the performance similar to the mileages that a car runs before breakdown. Mechanisms with minimum moving parts have an advantage both in terms of lifetime and replacement of parts. By doing so, we could increase the durability of the system. We assigned this criterion a weight of 12.5.

- **Safety Measures (22.5)**

  The safety of the user was given prior consideration throughout wearable industries. However, skin pressure sores and injuries persist. As these devices interact with and among human beings, we considered to include this criterion in our study. The safety of the mechanism has been addressed [28], [8]. We considered injury scenarios such as falling situations, hurting areas, sharp corners, pinch points, hoist supports, crutches, power failure joint release mechanism, and power failures modes during the design to ensure no or minimal injury. One of the essential criteria that we concluded from this function was to incorporate a Normally-Closed type actuation to ensure user safety during a power failure. We assigned this criterion a weight of 22.5.

- **Output Holding Torque and Testing (22.5)**

  The idea for the HEX GEN-1 was to execute a phased build to achieve multiple activities. Hence, in this path, the current knee was designed to achieve level-ground walking. The dynamic and static holding torque parameters are fundamental requirements [12]. The testing procedure and tests carried out will enable researchers to understand the device better. We assigned this criterion a weight of 22.5.

- **Others (7.5)**

  The don/doffs times are essential features in the wearable community. The ability to don/doff is very important. Based on its popularity among the wearables, we assigned it a weight of 2.5. The design time for the exoskeleton was another key criterion that we considered during our design to maintain constant progress on our exoskeleton work. We assigned this criterion a weight of 5.

  For each mechanism, we assigned a value between 1-10 (1 being the worst, 10 being the best) for these criteria. These scores and weights were multiplied to calculate the total score of 1000. The comparison of these scores helped us choose and design an efficient system "the Wrap Spring Clutch/Brake mechanism" for the walking activity of HEX GEN-1. Fig 3.1 shows the result of the trade study.

	Metrics	Weight	1	2	3	4	5	6	7	8	9	10	11	12
2	Options:		Wrap Spring	Motor	FES Only	Gears, Clutch	Linkages , Cable	Series Elastic Actuator	Hydraulics	(MR)Brake	Drum Brake	Belt and Hammer	Magentic Damper	Wafer Disc Brake
3	Manufacturing Cost	10.00%	10	2	10	1	9	4	5	5	7	8	4	7
4	Mehanical Mass	15.00%	10	2	9	8	9	5	2	6	5	7	5	7
5	Power requirements	10.00%	8	2	4	8	10	2	2	5	6	8	6	8
6	Lifetime/Service	12.50%	6	8	8	9	9	8	8	9	7	7	9	7
7	Time needed for Don and Doff	2.50%	9	9	8	9	7	5	5	8	7	7	7	9
8	Safety Measures	22.50%	8	10	10	7	0	7	7	10	8	7	10	10
9	Design time needed	5.00%	9	6	8	5	8	6	6	5	7	7	5	7
10	output holding torque	22.50%	8	8	0	10	8	7	8	8	7	7.5	9	8
11	TOTAL SCORE	100.00%	80	80	80	80	80	80	80	80	80	80	80	80
12														
13	GIVEN SCORE	1000	832.5	627.5	660	752.5	675	592.5	580	752.5	682.5	731.25	757.5	805

Figure 3.1: Trade Study

3.2 Biomechanical Factors for Designing

Fig. 3.2 and 3.3 shows the maximum range of movement of knee joint during sit to stand transition and walking. For normal activities such as sit to stand transition and level ground walking, the maximum angle observed is less than 110^0 so a value of $0 - 105^o$ can be chosen for the range of motion. The torque values from the motion capture system and the literature showed that the holding torque value at the knee joint for ground level walking doesn't exceed 50Nm. Hence this value was chosen as the design target for the system. Table 3.1 mentions the range of

motion and torque values based on which the exoskeleton was designed

fig 3.2, 3.3 shows the data collected during human trials using..

Bio-Mechanics of joints			
Joint	Flexion	Extension	Torque
Hip	$-110°$	$30°$	60N
Knee	$-105°$	$0°$	50N
Ankle	$-20°$	$45°$	-

Table 3.1: Joint limits

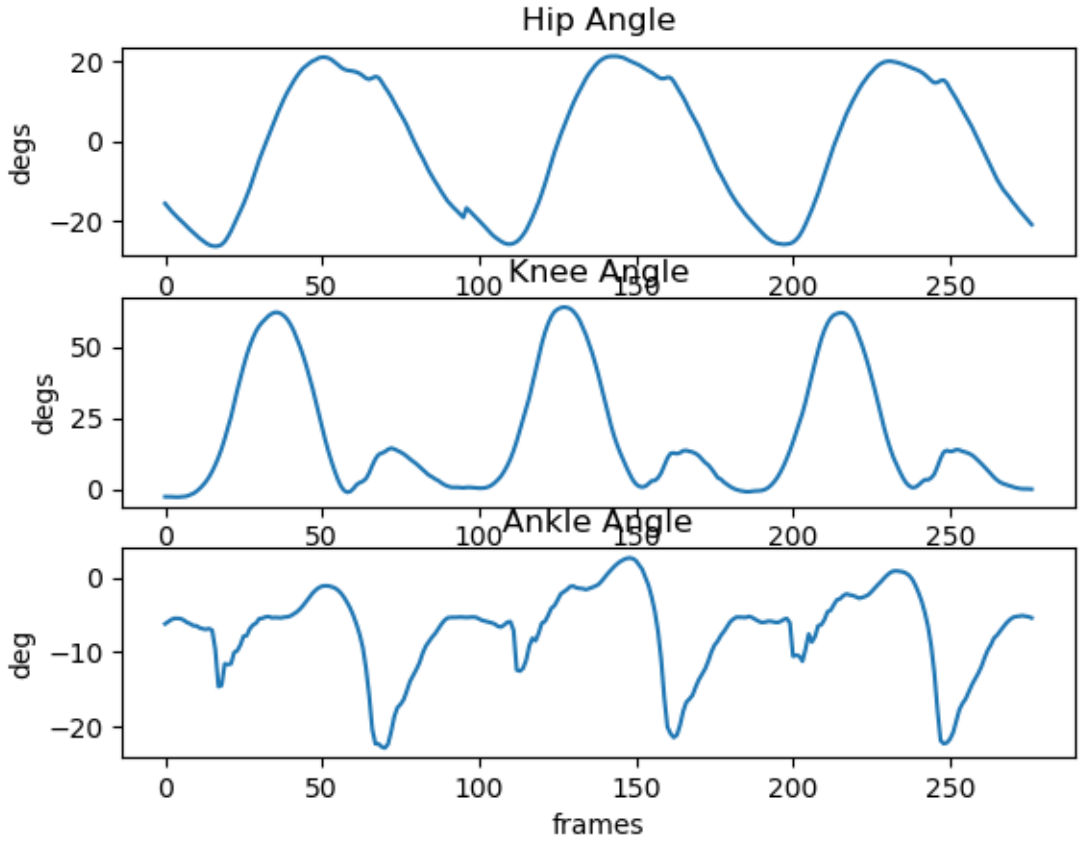

Figure 3.2: Healthy human walking trial

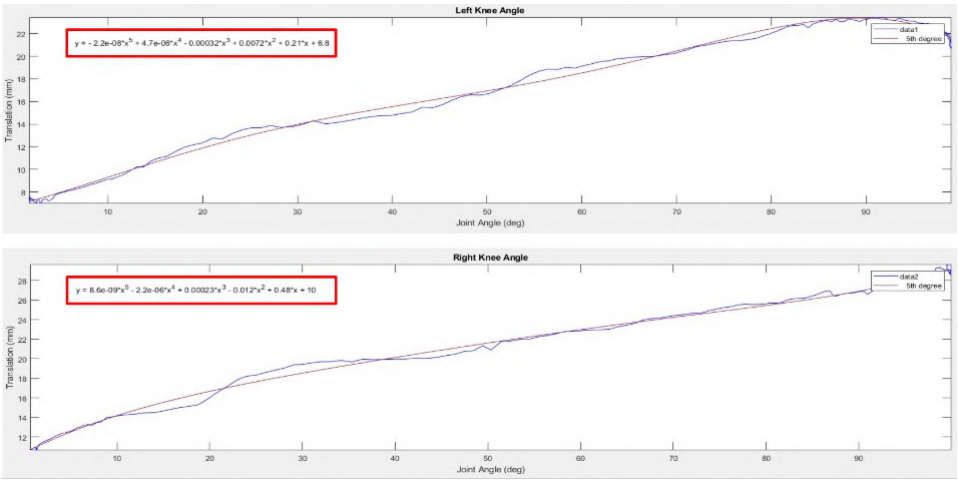

Figure 3.3: Healthy Human Sit to Stand Trial

3.3 Wrap Spring Mechanism

After the human trials and trade study we had solid information about the joint's range of motion and holding torque. Based on the results we decided to choose the wrap spring clutch/brake mechanism due to its quasi-passive nature, weight and cost of manufacturing.

When the legs of the torsion spring are brought together the inner diameter of the torsion spring reduces and when they are moved apart the coil diameter increases. If an arbor is placed inside this spring as shown in fig. 3.4 and when the legs are close together the spring wraps around the arbor making it harder for the arbor to move , but when the spring legs are moved apart as shown in the bottom figure, there exists no interaction or a small gap between the arbor and the spring which results in free movement of the arbor.

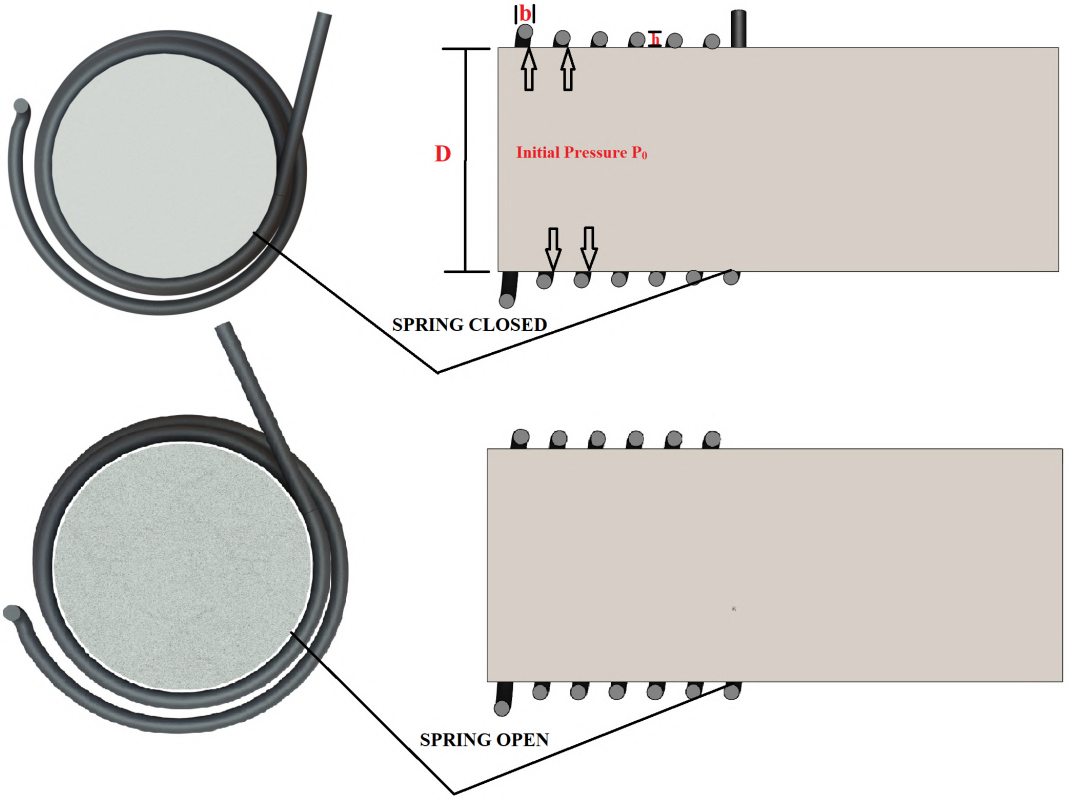

Figure 3.4: Wrap Spring Brake Open and Close

3.3.1 Torque and Pressure Equations

The design and shape of the spring plays a major role in deciding the frictional parameters and contact pressure of the mechanism. Papers or journals in the past have no references to how these equations were derived or how it affected the relationship. The formulae governing the torque and pressure were mentioned in [33] and [26].

$$T_0 = \frac{p_0 b D^2}{4}(e^{\mu\Phi} - 1) \qquad \text{Holding Torque} \qquad (3.1)$$

where

T_0 = Output Torque

p_0 = Initial Pressure

b = Spring Width

D = Arbor Diameter

μ = Frictional Coefficient

ϕ = angle (covered by the area)

$$p_0 = \frac{8EI\delta}{b(D+h)^4} \qquad \text{Initial pressure} \qquad (3.2)$$

where

E = Young's Modulus of Spring Wire

I = Moment of Inertia of Spring Wire

δ = Diametric Interference between Arbor and the Spring

h = Spring Height

Hence to establish this relationship we retraced the steps to its fundamentals .

3.3.2 Concept behind the Mechanism

The basic working principle behind the wrap spring is similar to that of a band brake and capstan friction and most of the equations of the system are derived from it. In a wrap spring clutch, the torque in the first coil is amplified exponentially across each successive coil due to frictional forces developed during the rotation.

The diameter of the arbor is made to be larger than the inner diameter of the spring to establish an interference between these two components. This creates an initial contact pressure and when rotated the frictional coefficient and this initial pressure causes a frictional force between the parts.

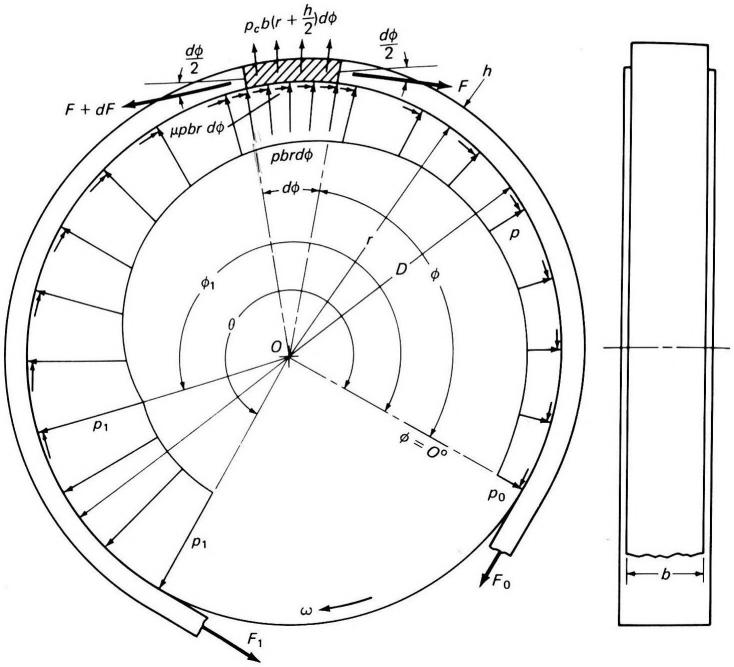

Figure 3.5: Band Brake Representation [6]

Fig 3.5 shows a 2d representation of how pressure is distributed across the drum. A 3d representation of pressure distribution on the spring is shown in fig 3.7 on the end of this section.

3.4 Equations governing the wrap spring clutch/brake

The derivation process involved references from the book [6] and [33]. The holding torque of a band brake is given by the following equation.

When a pressure is applied over an area of brdΦ the normal force equals to pressure times the area which gives us a value of pbrdΦ.

where the following values are represented in fig. 3.5

p = total pressure

b = breadth of the wire

r = radius of the arbor

$d\Phi$ = small area

When the body starts to rotate the frictional force in the system is estimated using the frictional coefficient and the normal force which turns out to be pbrd$\phi * \mu$.

This force is applied tangentially to the radius of the arbor which results in a torque thus giving us the torque equation to be r* pbrd$\phi\mu$.

When we calculate the normal and tangential forces from the Fig 3.5 we get the following equation

$$p = p_0 e^{\mu\Phi} \qquad \text{Pressure Equation} \tag{3.3}$$

when it is integrated over the area the following torque equation is obtained.

$$\begin{aligned} T_0 &= \int_0^{\phi} r(\mu p b r d\Phi) \qquad \text{Torque Equation for band brake} \\ &= p_0 b r^2 \mu \int_0^{\phi} e^{\mu\Phi} \\ &= p_0 b r^2 (e^{\mu\Phi} - 1) \end{aligned} \tag{3.4}$$

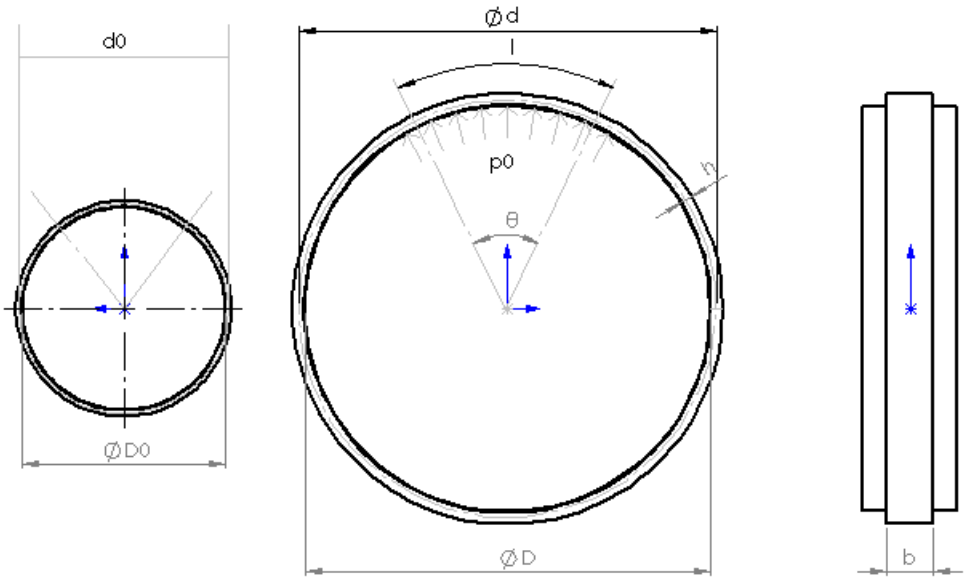

Figure 3.6: Mechanism behind wrap spring clutch

The initial pressure p_0 on the coil is a function of material property, moment of inertia, Flexural Rigidity (EI) of the spring, diametric interference (δ) between the coil and the arbor , and the diameter (D) of the arbor and is derived as follows, the force on the area bRθ does the following work.

$$dU = (p_0 dr)(bR\theta) = (p_0 dr)(bR\frac{l}{r}) \tag{3.5}$$

where the following values are represented in fig. 3.6

dU = Work

θ = angle covered by the area

r_0 = mean radius in fig 3.6

and the total energy stored when the moment is uniform is estimated using moment of

inertia of a curved beam

$$U = \frac{EIl}{2r_0^2}(1 - \frac{r_0}{r})^2 \tag{3.6}$$

where the following values are represented in fig. 3.6

U = Energy

l = Length of the Arc

The derivative of the above equation with respect to the median radius states the work and by equating 3.6 and 3.5 we get the value of p_0 to be

$$p_0 = \frac{EI(r - r_0)}{bRr_0r^2} \qquad \text{Initial pressure}$$

The assumptions such as $r_0 = R = r = \frac{(D+h)}{2}$

$$p_0 = \frac{8EI\delta}{b(D+h)^4} \qquad \text{Initial pressure Equation} \tag{3.7}$$

by replacing the value of p_0 in the pressure equation, the pressure equation changes to

$$p = \frac{8EI\delta}{b(D+h)^4}e^{\mu\Phi}$$

Combining the pressure and torque equations we get the output torque to be

$$T_0 = \frac{2EID^2\delta}{(D+h)^4}(e^{2N\pi\mu} - 1) \qquad \text{Holding Torque}$$

where

$\Phi = 2N\pi$

N = Number of Coils

Thus from this detailed procedure the torque and pressure relationship can be well understood and further changes can be implemented to the mathematical model to create any new relationships.

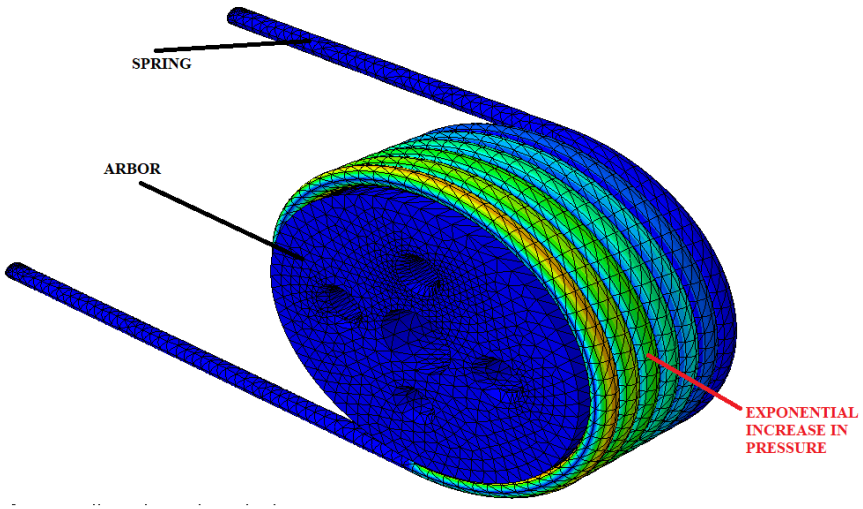

Figure 3.7: 3D representation of pressure distribution on the spring

3.5 Mathematical Modelling for Parameterization

A mathematical model of the system was created to estimate the optimum interference values for the specified holding torque. This can be calculated using the equations from the previous section. The model was executed in MATLAB and subsequent steps can be followed to replicate the design,

STEP 1: DETERMINING INITIAL PARAMETERS

For the current system a torque value of 50 Nm was decided. Most of the stock available

torsion springs had diameter less than 1.5 inches, hence we planned on using a custom spring for our model. Based on aesthetics and weight limitations we decided the upper bound value for the spring diameter and thickness to be 2 and 1 inch. The most common material used to manufacture spring was music wire and we chose the same material for our application. A wire diameter of .115 inch was chosen which in the later steps were tested for stress limitations and factor of safety. With these parameters we progressed to the next step.

STEP 2: SPRING WIRE DIAMETER CALCULATION

For the specified load value a minimum spring wire diameter can be calculated using the maximum tensile stress equation and the force torque relationship.

$$\sigma = \frac{load}{Area} \qquad load = \frac{torque}{radius_{arbor}} \tag{3.8}$$

where

σ = stress by combining the above two equations we get

$$\sigma = \frac{torque}{Area * radius_{arbor}}$$

substituting the values of torque, arbor radius and the maximum tensile strength of the spring material, the minimum wire diameter was calculated. Then a new stress was calculated for .115in diameter wire. Factor of Safety for the stress was calculated by dividing the new stress and the Young's modulus.

$$FOS = \frac{Young'sModulus}{CalculatedStress}$$

STEP 3: CALCULATING UPPER AND LOWER BOUNDS FOR INTERFERENCE
To estimate the interference value between the arbor and the spring the Holding torque equation was used. For the lower bound interference, the number of active coils was decided based on maximum knee joint thickness and the spring coil diameter. For this configuration the maximum value of N was 6.5.

From [33] we found that the use of kinetic friction coefficient was preferred rather than static due to the movement in the arbor.

The arbor diameter can be written as a function of spring's inner diameter and the diametric interference. Hence by substituting these values into the equations we got the lower bound value for diametric interference.

The upper bound interference was calculated using the Overrunning torque. Generally, the resistive force value in the extension direction should be zero but literature showed that a value upto 10 lb-in didn't have a major effect on the walking gait. So we chose a smaller value and repeated a similar approach to find the upper bound value for diametric interference using the following equation.

$$T_U = \frac{2EID^2\delta}{(D+h)^4}(1 - e^{-2N\pi\mu}) \qquad \text{Overrunning Torque} \qquad (3.9)$$

Based on the upper and lower bounds, a value in between can be chosen as the diametric

interference for the design is used to define the arbor diameter. So by the end of the mathematical model we had a solid value for which we designed the knee joint.

Spring Coil Inner Diameter - 1.7158 in

Spring Wire Diameter - 0.115 in

Number of turns - 6.5

diametric interference - .0277 in

Arbor Diameter - Spring Coil Inner Diameter + diametric interference - 1.7435 in

Chapter 4

Hardware Design

4.1 CAD Modelling

The Knee joint comprises of two subsystems the thigh and the shank, where the former was considered to be fixed and latter as the moving joint.

The end cover houses the bearing for double support and acts as a clamp to align the center of the spring with the arbor which can be seen from fig. 4.1. A solenoid was mounted on the thigh link to engage and disengage the clutch.

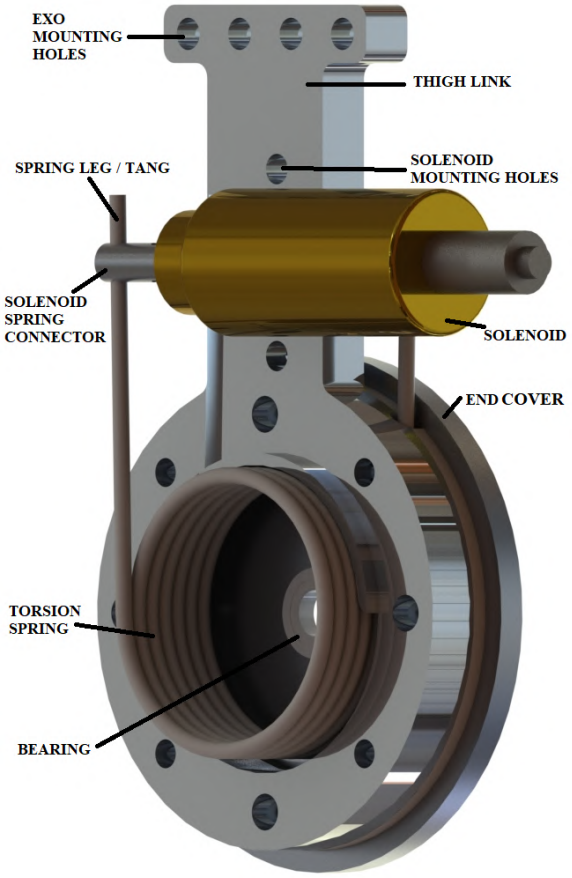

Figure 4.1: Thigh Assembly

The arbor and the shank link were designed as separate parts for ease of manufacturing. A center shaft has a press fitted bearing on one end and a close fit bearing on the other. The shaft is coupled to the arbor via a set screw. The shaft has a hollow center to mount a potentiometer.

The shank assembly shown in fig. 4.2 is pushed into the spring and the end covers are bolted.

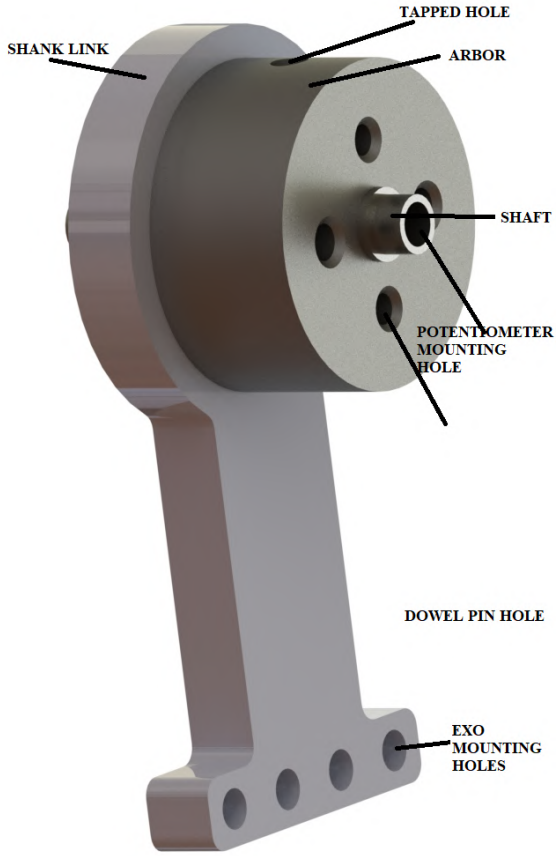

Figure 4.2: Shank Assembly

Parts other than the arbor, shaft and spring are made out of Aluminum 6061 and the arbor and shaft are made using 8620 steel. The mountings for potentiometer, solenoid and the casing are 3d printed to make the exoskeleton lighter.

Studies and literature have used large diameter hollow center hole for weight reduction, but our design uses a solid arbor.

The exploded view of the knee joint is shown in 4.5 and the assembled joint is shown in 4.4.

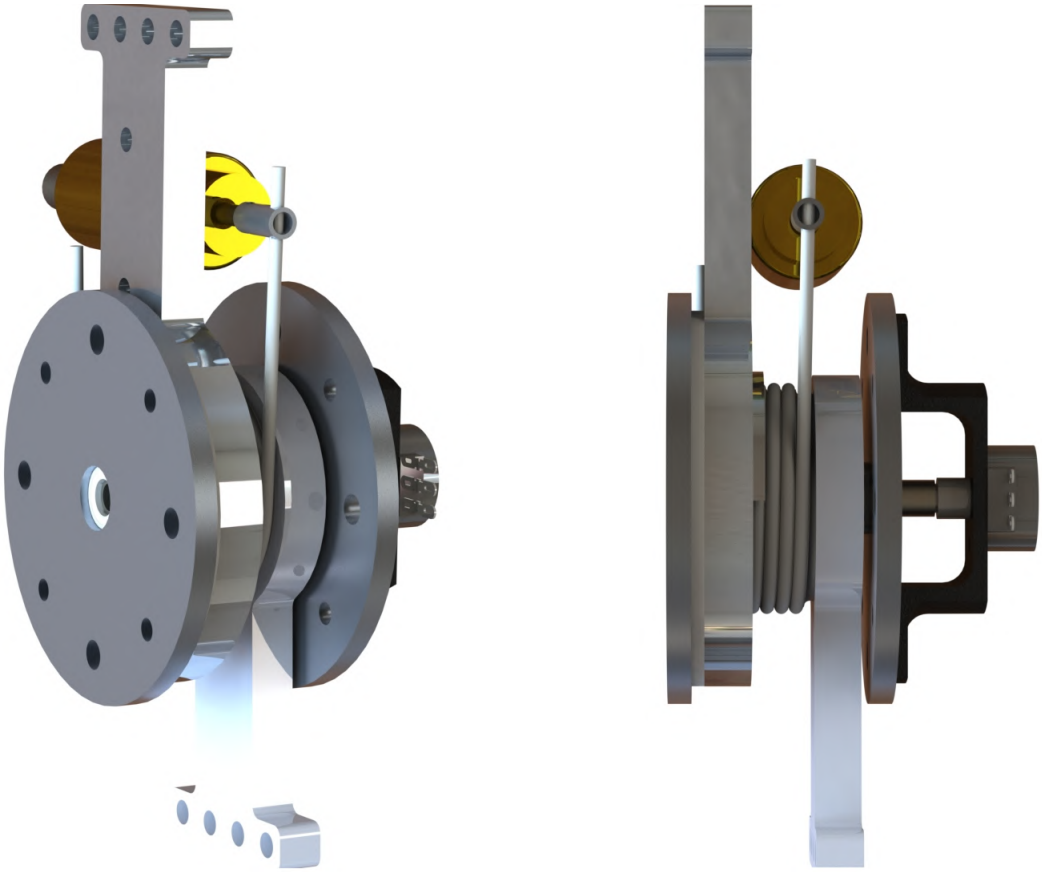

Figure 4.3: Assembled and Side View of Knee Joint

Figure 4.4: Rendered Image of the Knee Assembly

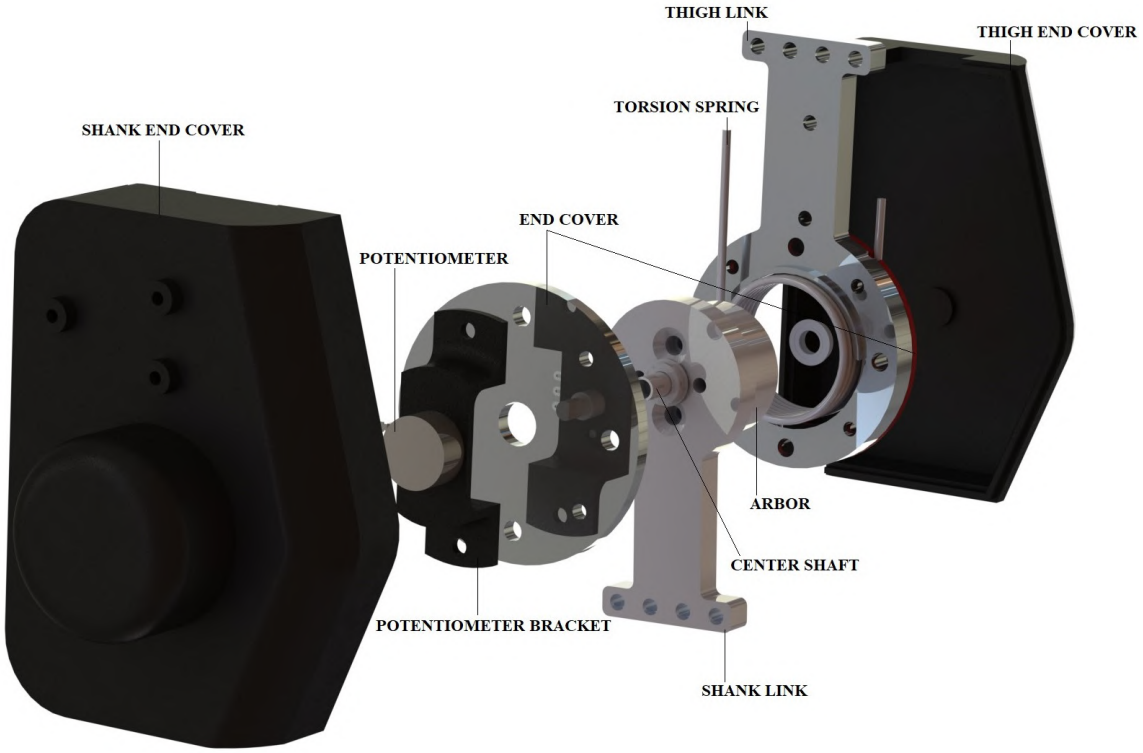

Figure 4.5: Rendered Image of Knee Exploded View

4.2 TEST BED SETUP

Fig 4.6 shows the extension set up. The end of the shank link is connected to a rope - pulley system. At the end of the rope a loadcell is connected to measure the load values.

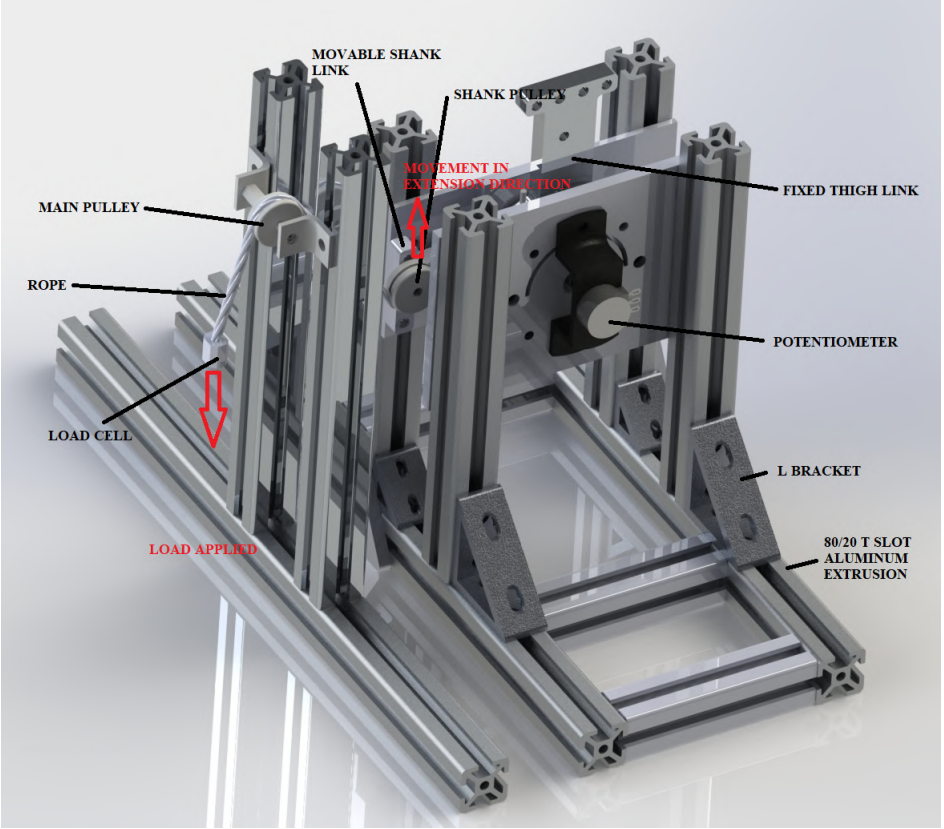

Figure 4.6: Rendered Image of Extension Test Rig Set up

Fig 4.7 shows the test bed for knee flexion test. The longer leg length provides greater torque values.

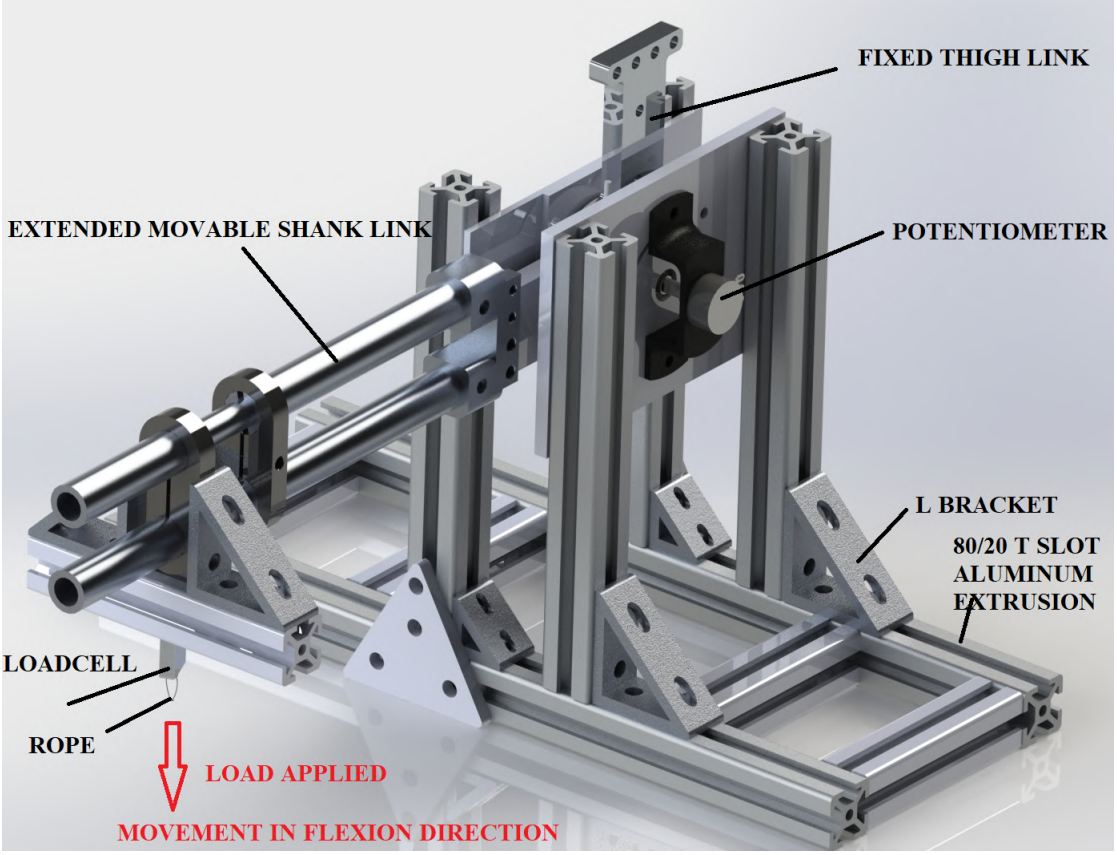

Figure 4.7: Rendered Image of Flexion Rig Set up

4.3 Model for Simulation

A simple model was created in SolidWorks and the file was saved in a .igs format to import the model into Abaqus. The SolidWorks includes the interference which means that there will be an overlap in the design. The rotational angle from the testing is used in the simulation. This is specified in the abaqus software.

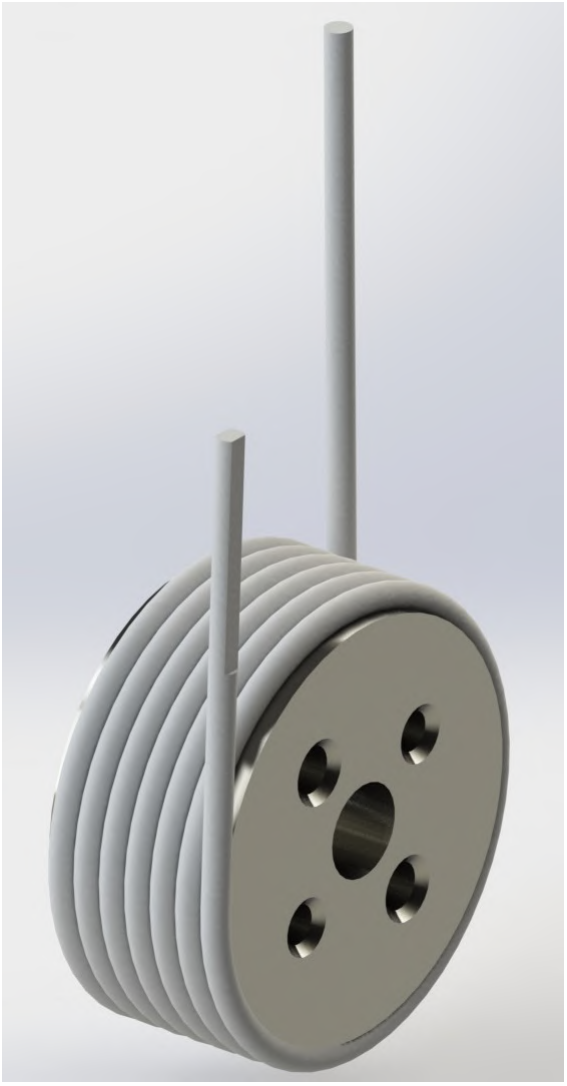

Figure 4.8: Simulation CAD Set up

The simulation is used for studying the optimization of the mechanism. One of the main challenges in running an analysis for this type of system is defining the contact properties. And since the contact is changing continuously, right specifications and right size and shape mesh elements must be created. A detailed procedure is stated in the simulation chapter of the thesis.

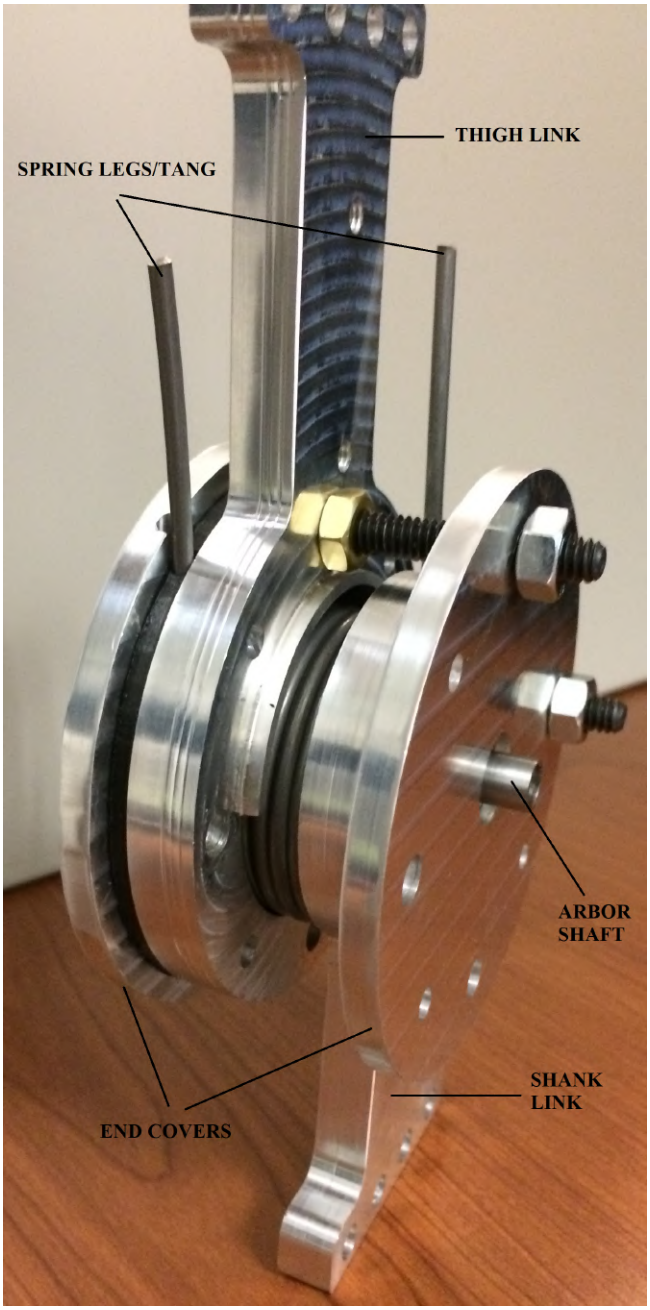

(a) Assembled Knee Joint after Manufacturing

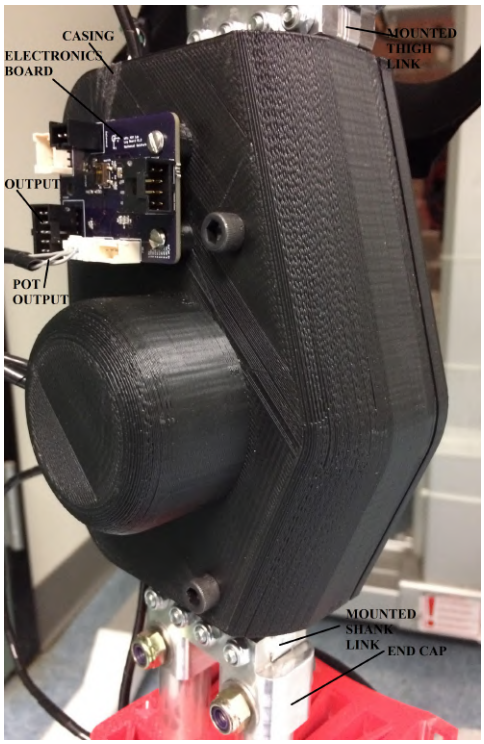

(b) Knee Joint on the Exoskeleton

Figure 4.9: Knee Joint of HEX GEN-1

4.4 Other Manufacturing Work

After completing the machining process of the Knee joint, I carried out the manufacturing of the adjacent parts which connect different joints of the exoskeleton using CNC Machines. The parts include End Cap, Connecting tubes and Tube Clamps. The strap carriage couples the exoskeleton to the human body. This was 3d printed using Luzlabot 3d printer with an infill density of 75 percentage. The density had to be this large to ensure mechanical safety of the system.

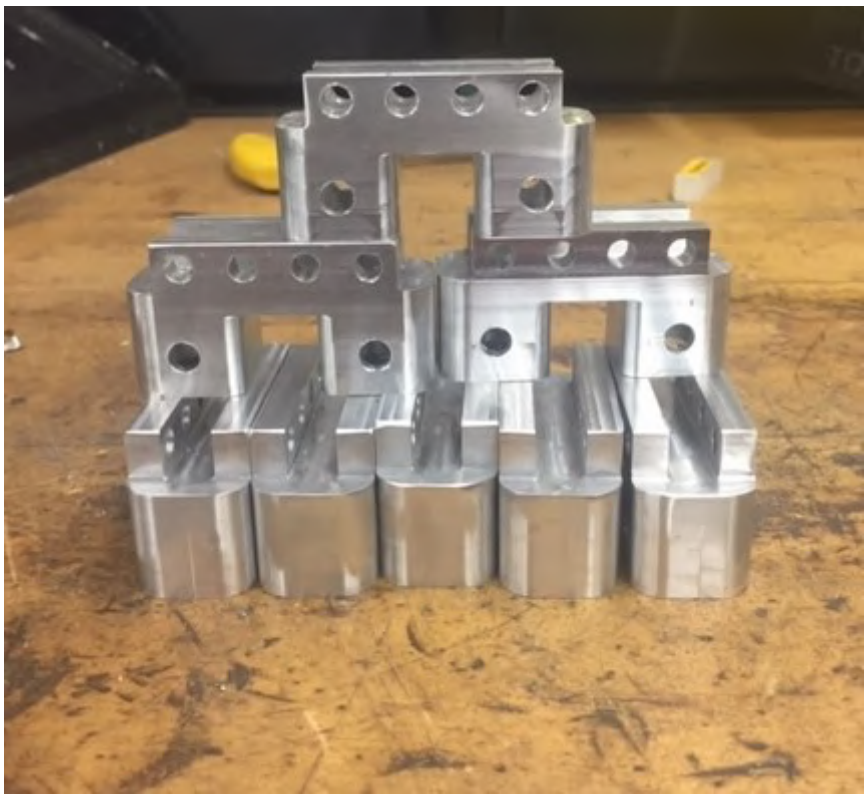

Figure 4.10: End Caps coupling the joints to the cylindrical tubes

Figure 4.11: Pipe Clamps are used to clamp the inner rigid rods with the hollow tubes

The full body assembly of the exoskeleton after manufacturing is shown in fig 4.12

(a) Assembled Exoskeleton Front View

(b) Assembled Exoskeleton Side View

Figure 4.12: HEX GEN-1

Chapter 5

Testing

5.1 Types of Testing and Reasons

EXTENSION FRICTION and TANG MOVEMENT TEST

The primary reason behind this test is to study the relationship between normal force and the interference to estimate the initial pressure on the system and the minimum force required to move the joint in the knee extension direction.

FLEXION HOLDING TORQUE TEST

This test was conducted to study the dynamic nature of the knee. The knee joint was loaded and the brake was engaged for a particular time interval and after which it was released. These cycles were repeated to check if the brake engages in the same starting position.

LOSS IN RANGE OF MOTION TEST

Literature have mentioned that after continuous overloading of the system there will be a hysteresis in the spring due to plastic deformation. No quantitative data were mentioned in the literature. To estimate the amount of loss this test was executed.

RELEASE TEST

Before selecting an actuator to release the mechanism, data such as actuator force and deflection must be known. To learn about these details we conducted this test where the loadcell was connected to the free end of the spring leg which was pushed to estimate the force value.

5.2 Setup for Extension Testing

5.2.1 Extension Friction Test with no tang movement

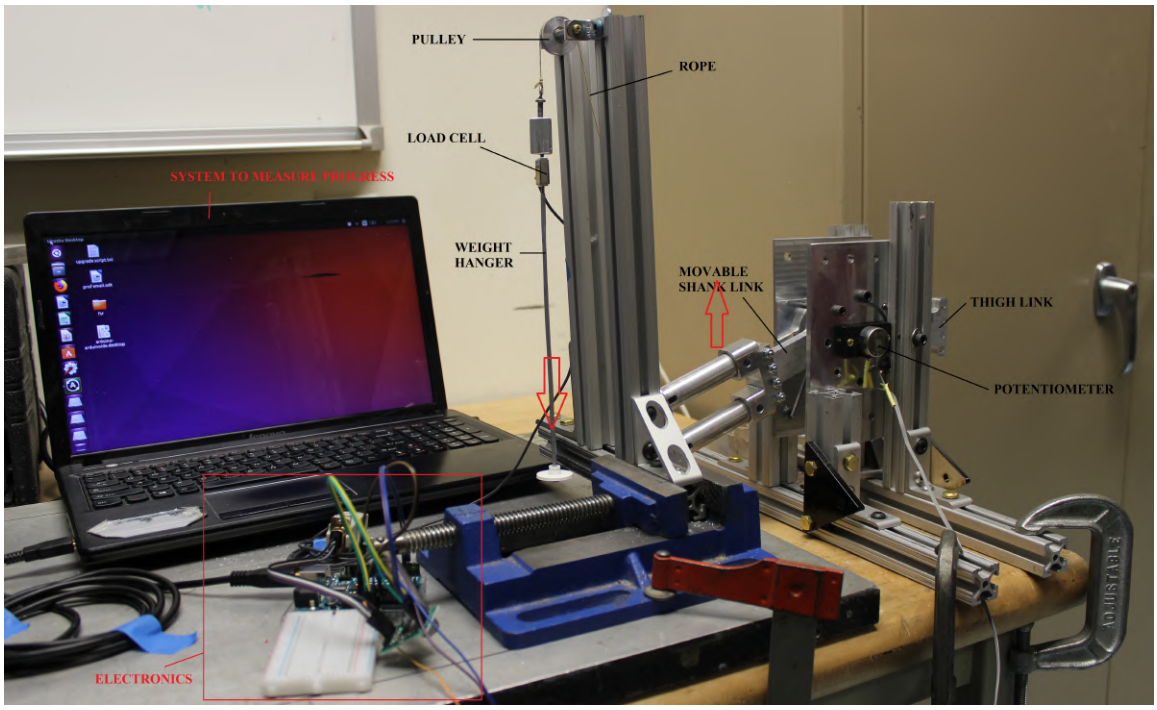

Figure 5.1: Extension Test Rig Set up

5.3 Setup for Extension Testing

The data from the load cell and potentiometer were read using an arduino. Initially the weight scale was calibrated and during the test, weights were added and the movement of the shank link in the extension direction was studied. After a particular weight limit the shank link started slipping. The data from the sensors gave us the exact load value at which the slipping happened. This force value was used to estimate the contact pressure value at which the slip happened.

5.3.1 Extension Friction Test based on tang movement with definite intervals

The above test was carried out at zero tang movement. But we wanted to learn the relationship between spring opening and contact pressure. The diameter of the spring was changed by pushing the free leg of the spring and for this new position the above testing was repeated. A similar process was repeated for different diameter of the spring opening.

5.4 Setup for Flexion Testing

5.4.1 Holding Torque Test

A similar approach to that of the exoskeleton's height adjustment was followed to increase the shank link's length during the flexion test. This gave us a wide range of lengths at which we were able to load the knee joint

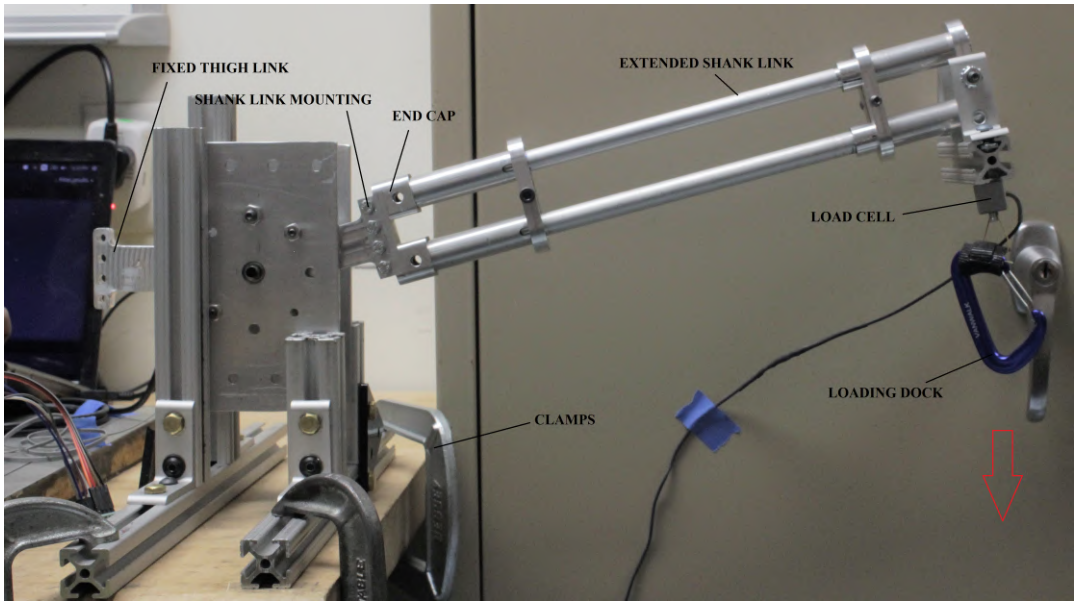

Figure 5.2: Flexion Test Rig Set up

Chapter 6

Simulation

6.1 Reasons for Simulation

The data from the physical testing for knee extension determined the point of deflection as a function of load.

The value obtained during the testing can be verified using the simulated model. Simulation also allows for ways to optimize the design which during the testing is time consuming. The simulation was executed in ABAQUS which is a FEA software and the steps to simulate the model are explained in the following section.

6.2 Steps For Simulation

STEP 1 : MODEL IMPORT

The first step is to import the SolidWorks model into the software. To do so, the explicit/dynamic analysis was selected in the ABAQUS software. Right click the part session to import the file.The Solidworks file were converted to IGES format for the

import.

STEP 2 : MATERIAL PROPERTIES AND ALLOCATION

The next step is to create material properties and to assign these materials to the consequent parts. A simple arbor spring mechanism was used to run the simulation. The material properties for the spring and arbor are as follows

8620 Steel

CREATE MATERIAL - GENERAL - DENSITY - Assign the value to be 7.85e-9 g/cm^3 - MECHANICAL - ELASTIC - Assign the Young's modulus to be $205 * 10^3$ Mpa and poisson's ratio as .29

Music Wire

CREATE MATERIAL - GENERAL - DENSITY - Assign the value to be 7.85e- $tonne/mm^3$ - MECHANICAL - ELASTIC - Assign the Young's modulus to be $210 * 10^3$ Mpa and poisson's ratio as .313

Assign the material to the particular part.

STEP 3 : ASSEMBLY

Assemble the files based on your requirement using instances such as translate, rotate. etc.,

STEP 4 : STEPS

The step time for the simulation is mentioned in this particular session. For our simulation two steps are included. One to simulate the expansion of the spring due to interference and the second step is to simulate the rotation. A static general approach was selected in this step because of the nature of the simulation. Mention the time period and the increment size. The increment size should be decided based on the number of mesh elements. A similar approach had to be carried out for the second step as well.

STEP 5 : INTERACTION

For the simulation of wrap spring clutch/brake mechanism this step is particularly important. The interaction properties must be created for both the steps. For step 1 the tangential behavior is set to frictionless since it simulates the expansion of the spring due to interference. CREATE CONTACT PROPERTY - CONTACT - MECHANICAL - TANGENTIAL BEHAVIOR Using a similar approach after creating the second interaction property for step 2 specify the tangential behavior to be penalty and specify the frictional coefficient to be .15.

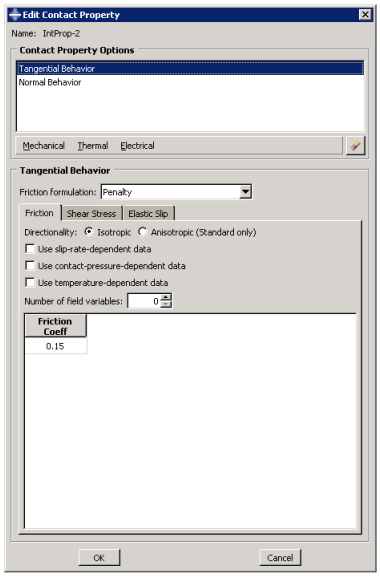

Figure 6.1: Interaction Property

Then a surface to surface interaction is created between the inner face of the spring and the outer surface of the arbor.

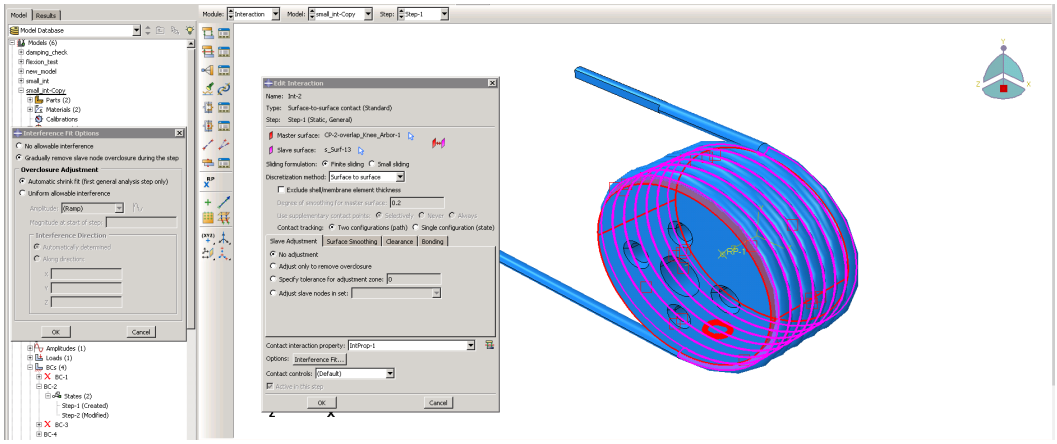

Figure 6.2: Surface to surface interaction

As an additional change a contact control must be created to simulate the damping and to specify how the control is executed. This is active during the first step and is inactive during second step. The contact control has an automatic stabilization factor 1 and tangent fraction of 1.

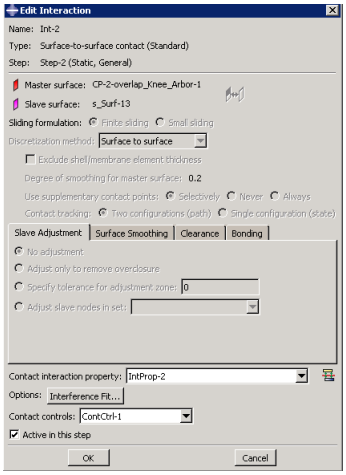

Figure 6.3: Contact Control

The next feature to include is the constraint. A reference point is created at the center of the arbor and a coupling constraint is used to couple the point to the surfaces of the arbor. This point can be later used to define the rotation/displacement of the arbor.

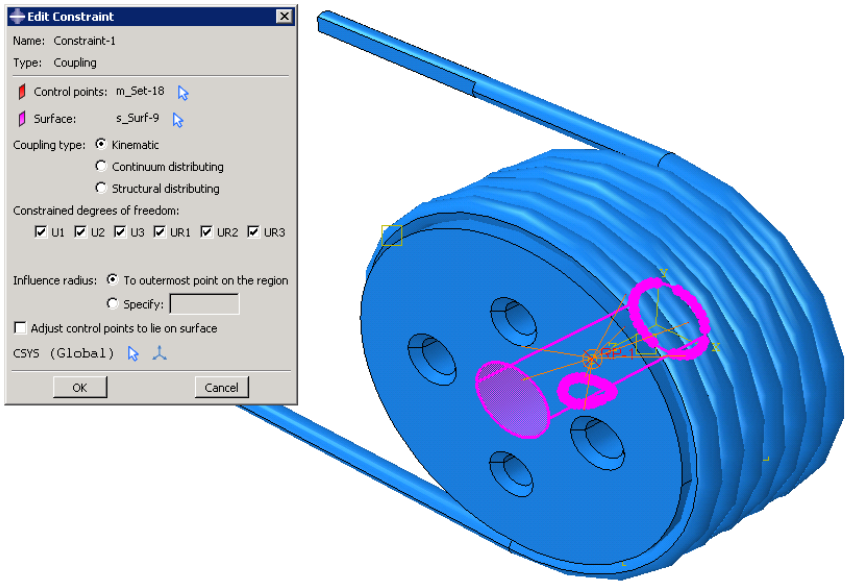

Figure 6.4: Coupling Constraint

STEP 6 : LOADS

Under this tab choose the boundary condition features to specify the movement constraints for system based on the step. Two boundary conditions were created one specifying displacement/rotation and other mentioning the encastre or fixed support. One of the advantages of using Abaqus is the control of joint movements based on step.

This was useful while specifying the rotation of the arbor. For the first step the rotation of the arbor was arrested but for the second step the rotation was given about the z-axis to cause the rotation.

STEP 7 : MESHING

Under this session initially the shape or type of mesh elements were set to tetrahedron which gave good approximation of mesh elements around the corner of the spring and the size of the elements were made finer for the spring due to its reaction to the loads. The size of the arbor elements were relatively larger.

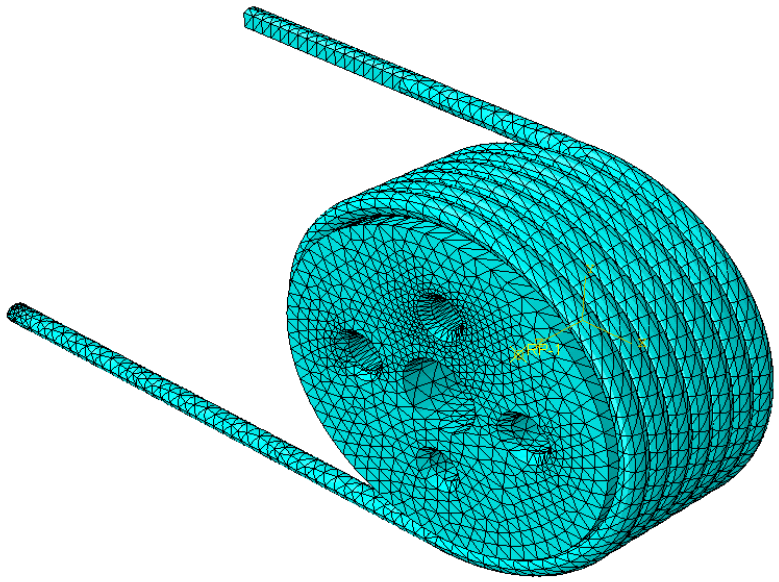

Figure 6.5: Mesh

STEP 8 : JOBS

A job was created for the specific type of simulation and the core parallelization was increased for faster simulation time and the results of the simulation can be viewed in the simulation session of the results.

Chapter 7

Results

7.1 Results

7.1.1 Mechanical Design

Table 7.1 reports the mass of the theoretical (CAD) and manufactured parts with a difference of 1.9 %. The total mass of the brake without the solenoid is $711g$. Hence our system stays within the predefined weight limit.

Parts	**Solidworks mass (grams)**	**Manufactured mass(grams)**
Arbor	244.15	243.0
Thigh Link	126.61	130.0
Shank Link	92.25	103.0
Arbor Shaft and Bearing	19.63	15.0
End Cover	2(80.11)	2(80.0)
Torsion Spring	54.87	60.0
Total	697.72	711

Table 7.1: Knee Joint Weight Distribution

7.1.2 Testing

By applying a force to the spring leg, we were able to control the inner diameter of the spring. This mechanism allows the interference value between the arbor and spring to be controlled as well. We carried our extension testing for five different interference values summarized in Fig 7.1. During our testing, we didn't measure the angular change during spring opening. If estimated, it can be used in Eq. 7.1 to estimate the new inner diameter and new the interference value at these different points. The black dots on Fig 7.1 represent the points of deflections for different spring openings. The $0push$ happens when the free spring leg is at its initial 0 position. $1push$ happens when the spring leg is moved horizontally by a distance of $.313in$ and so on until $4push$.

$$ID_{(new)} = ID(\frac{N}{(N \pm \theta)}) \tag{7.1}$$

where

ID_{new} = new loaded spring diameter

ID = relaxed spring diameter

N = Number of turns

θ = angle in radians between the legs of the spring

Fig 7.4, Fig 7.5 shows the results of the flexion testing. The red line shown in the plots represents the angle, and the blue lines represent the mass in grams. The brake engagement and disengagement phases are shown in the plots Fig 7.5a, Fig 7.5b.In Fig 7.5b for a period of time, the load stays at 120N, which states the brake engagement phase followed by which there is a drop in load, which signifies the disengagement phase.

Fig 7.4 shows the results of the durability test. During the test, the brake was engaged at three different loading conditions $48Nm$, $50Nm$, and $63Nm$. The brake was engaged

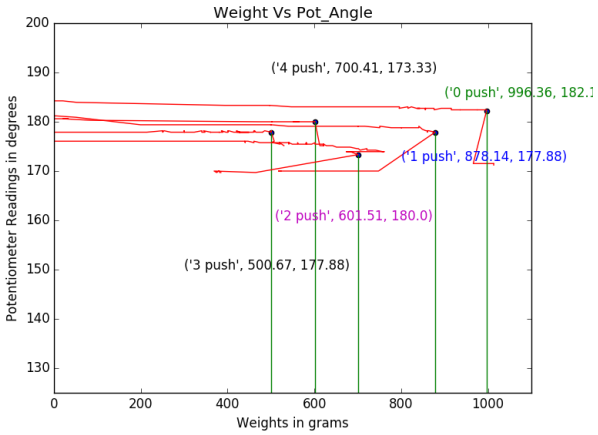

Figure 7.1: Slipping Load values during Extension Test

to hold this position for four consecutive days, where the load between the days were increased; $48Nm$ on the first day, $50Nm$ for the second and third (since being the target requirement), and on the fourth day, we pushed the brake to the peak value of $63Nm$. We observed an angular difference of 0.75^o on the final relative to the start of the test.

Fig 7.2 shows the angle lost after repeated peak load dynamic testing. The braking position has moved about (4^o) from its initial position. The peak value represents the initial braking position before testing, and the valley value represents the new position where the braking happens for the same load values. This difference was estimated to be the loss in the range of motion.

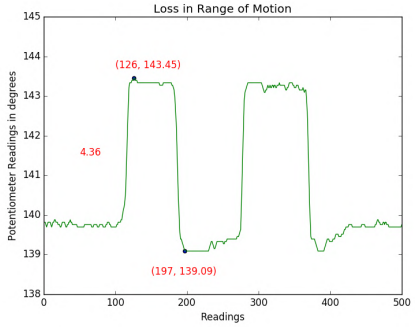

Figure 7.2: Loss in Range of Motion

Fig 7.3 shows the results of the brake release force test. The point depicted in Fig 7.3 represents the point of deflection, and the load value at this point ($2.5kg$) is the force

required by the solenoid on the tang to disengage the brake.

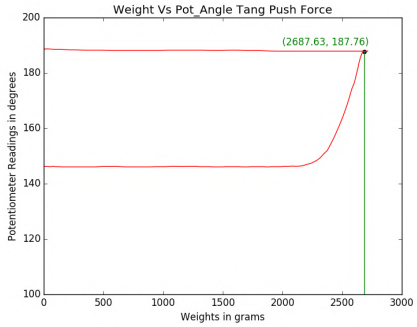

Figure 7.3: Brake Release Test

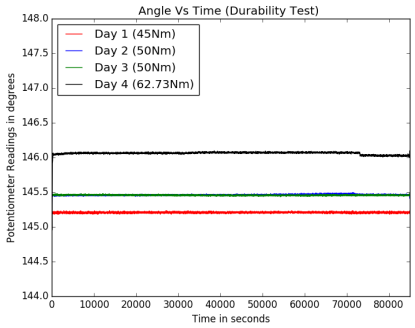

Figure 7.4: Durability Test

7.1.3 Trade Study

Based on our bill of materials, the cost to make a single knee joint is approximately $180, which does not include the cost to manufacturing. Based on this, we have shown that it is possible to build a low-cost quasi-passive knee joint that is lightweight and effective and which could execute ground-level walking. Fig 7.6, shows the range of motion of the knee, The range of motion achieved by the knee joint mimics the biological range of a knee. Our testing of the design, durability, and extension showed the endurance and safety of the knee joint.

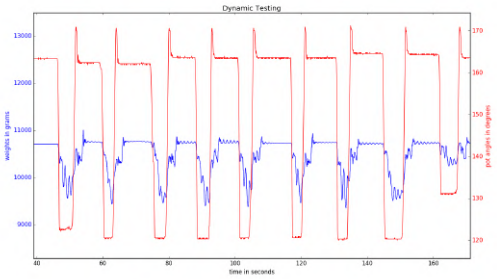

(a) Dynamic Testing result at 48 Nm

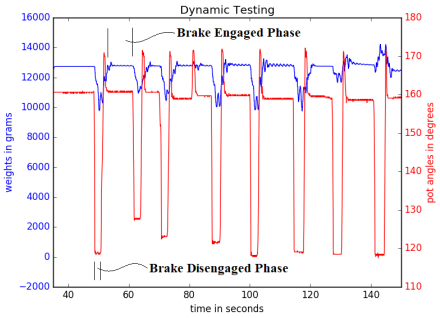

(b) Dynamic Testing result at 50 Nm

Figure 7.5: Flexion Testing Results

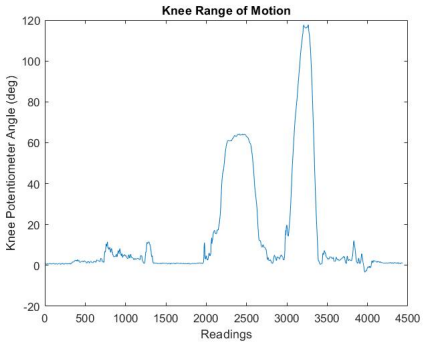

Figure 7.6: Range of Motion of Knee

7.2 Simulation

Optimization was carried out to estimate the Normal Force value based on the wire diameter, number of turns and interference values. This was executed for both Extension and flexion. The results of the simulation are as follows

The rapid growth in the torque value can be seen in the flexion simulation and the fall in force value can be seen in the extension. In the simulation for the first 0.5 s the system tries to reach the initial pressure value. In the next 0.1 s the value changes based on the rotation of the joint (extension and flexion). Fig. 7.7 shows that the force value drops as the interference increases.

Fig. 7.10 shows that the normal force or holding torque increases with interference value.

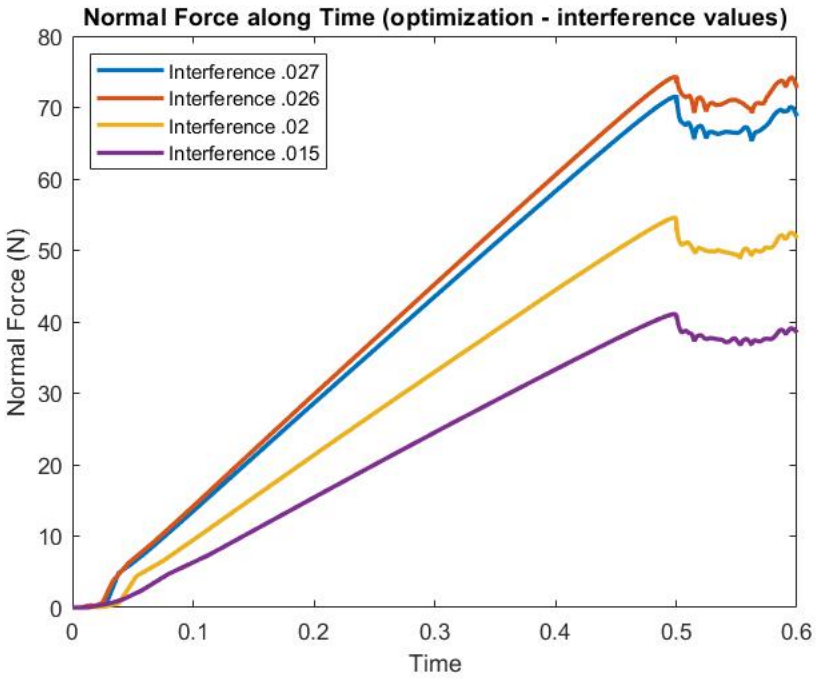

Figure 7.7: Optimization Based on Interference (EXTENSION)

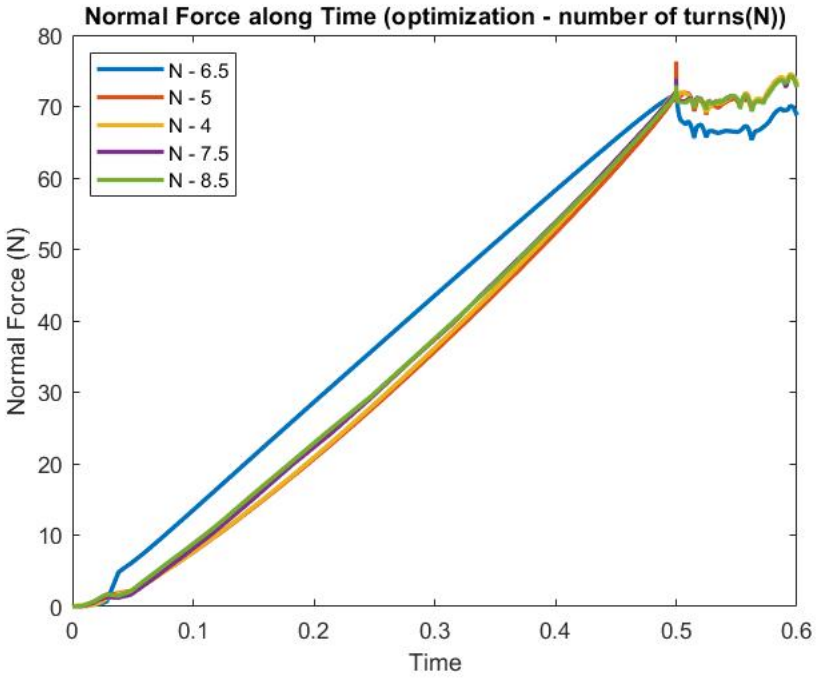

Figure 7.8: Optimization Based on Number of Turns (EXTENSION)

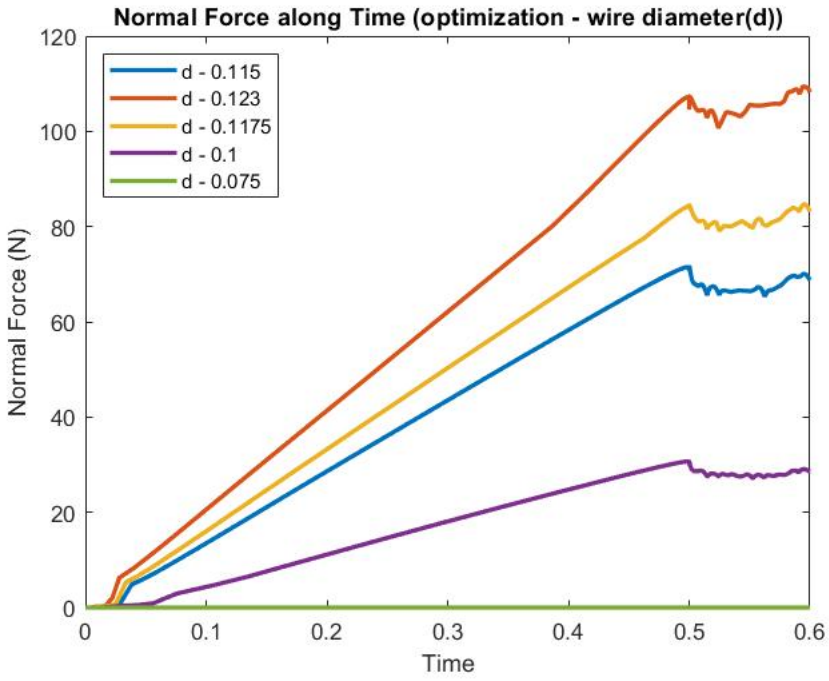

Figure 7.9: Optimization Based on wire diameter (EXTENSION)

But on the contrary fig 7.11 shows that changing the number of turns for the same size arbor doesn't affect the holding torque value. Fig 7.10 shows that by increasing the wire diameter a greater holding torque can be obtained.

So from fig 7.7, fig 7.10 shows that greater interference values can assist in greater holding torque but also has an adverse effect during knee extension. Hence an compromising value between the system has to be chosen for the best performance.

Fig 7.8, fig 7.11 shows that a torsion spring with minimum number of turns and longer pitch can have same effect as a torsion spring with larger number of turns and small pitch. The other key aspect which contradicts the mathematical equations is that increasing the number turns didn't have a major effect on the normal force value.

Fig 7.9, Fig 7.12 has a great effect on the normal force due to larger area of contact.

The simulation results states we can obtain a low weight, high holding torque and a

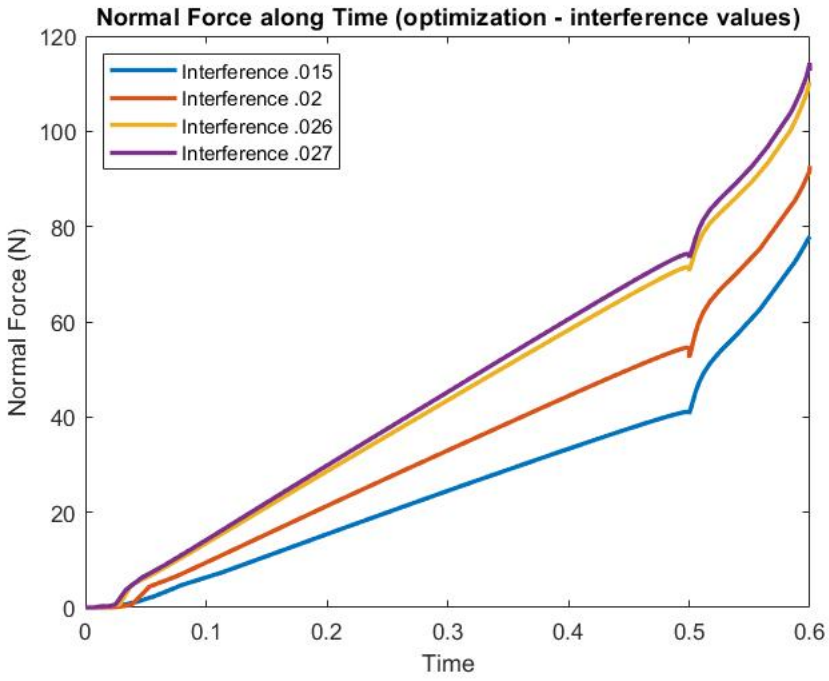

Figure 7.10: Optimization Based on Interference (FLEXION)

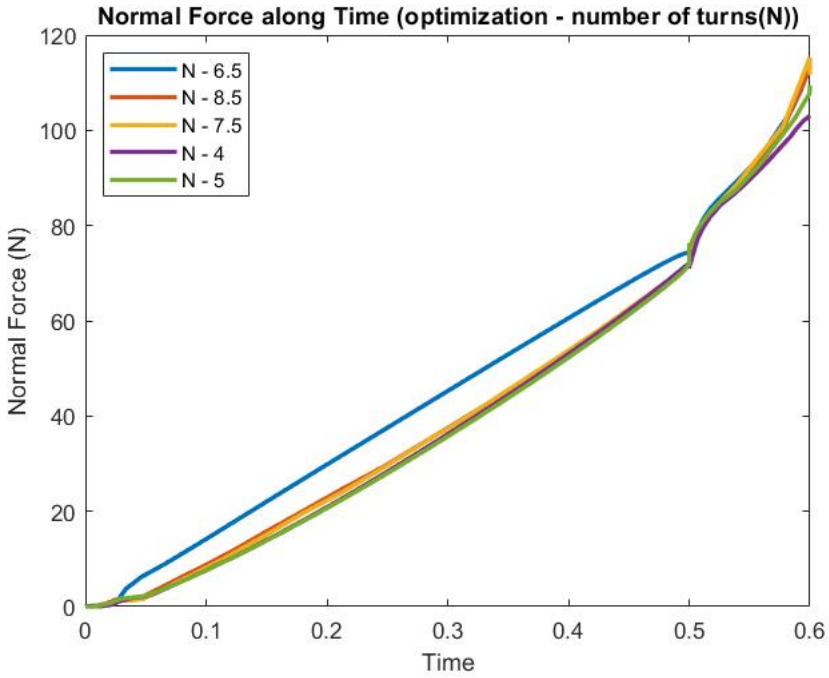

Figure 7.11: Optimization Based on Number of Turns (FLEXION)

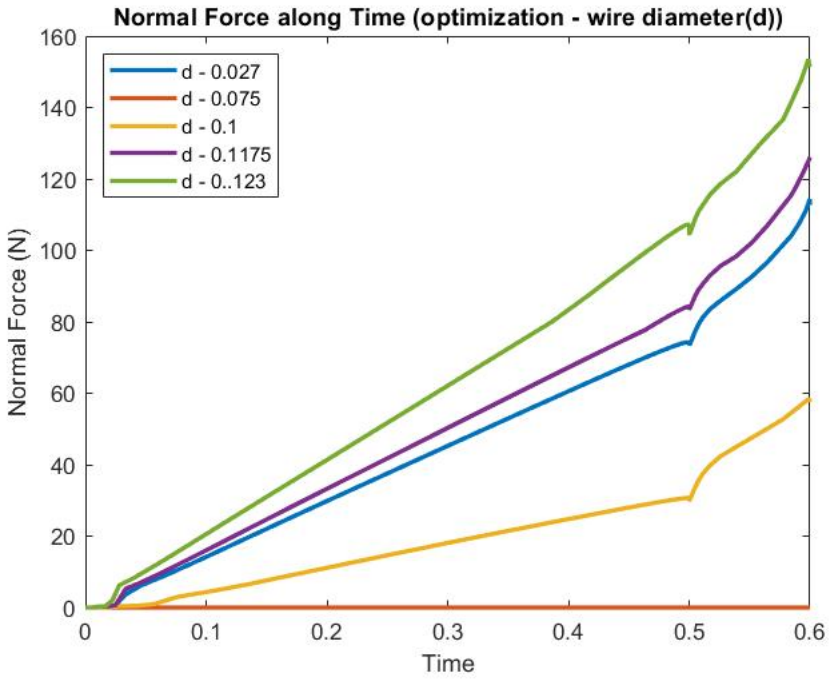

Figure 7.12: Optimization Based on wire diameter (FLEXION)

less thick system compared to the current one to achieve a high performance design for stair/ramp climbing.

Chapter 8

Future Work and Conclusion

8.1 Conclusion

Thus from this work we can conclude that the wrap spring clutch/brake mechanism can be used as a knee joint on an exoskeleton. The trade study approach can be utilized efficiently to track the status of a mechanism which can lead to development of existing mechanisms and to utilize a mechanism to its utmost potential. The analytical study will help future authors to implement or replicate a mechanism for other applications and to build devices around the mechanism which can be time consuming. The testing and simulation aspects can help determine to set goals for future tasks which can keep improving the mechanism until it reaches it saturation state.

The biomechanical way to design a knee joint and the results from the design and testing show that the system is capable to withstand the predefined loading condition that have been set for level ground walking and that the knee join can be optimized to match different holding torque values for different activities.

The design and assembly are currently being changed to include stair climbing activity.

During assembly it was hard to maintain a parallel structure between the end caps. To improve this, multiple spacer are placed around the end plate holes. Instead of clamping the spring at the very beginning there can be two mounting surfaces, one in the front and one after the first coil near the thigh link.

8.2 Future Work

Moving forward we are planning to execute human trials to learn about the system's behavior during continuous loading which will establish the working nature of the device.

As the next step I am eager to learn the characteristics of the threaded arbor which is a new design to improve the contact surface area between the arbor and spring and its weight bearing capacity. To do so a similar arbor with threads can be made and replaced in the test bed set up, and a similar testing procedure can be followed to study the characteristics. Incorporating such a major design change can lead to non-uniform pressure distribution and can cause varying frictional behavior across the surface. We are planning to study this new design to show its weight efficient and higher holding torque behaviour.

Bibliography

[1] Musa L Audu, Curtis S To, Rudi Kobetic, and Ronald J Triolo. Gait evaluation of a novel hip constraint orthosis with implication for walking in paraplegia. *IEEE Transactions on Neural Systems and Rehabilitation Engineering*, 18(6):610–618, 2010.

[2] Ekso Bionics. Ekso, 2015.

[3] Robert Bogue. Exoskeletons and robotic prosthetics: a review of recent developments. *Industrial Robot: An International Journal*, 36(5):421–427, 2009.

[4] Robert Bogue. Robotic exoskeletons: a review of recent progress. *Industrial Robot: An International Journal*, 42(1):5–10, 2015.

[5] Thomas C Bulea, Rudi Kobetic, Curtis S To, Musa L Audu, John R Schnellenberger, and Ronald J Triolo. A variable impedance knee mechanism for controlled stance flexion during pathological gait. *IEEE/ASME Transactions on Mechatronics*, 17(5):822–832, 2011.

[6] Arthur Houghton Burr. Mechanical analysis and design. *Elsevier North-Holland, xxvi+ 640, 26 x 19 cm*, 1981.

[7] Joshua Caputo. Humotech. https://www.humotech.com/products, 2015.

[8] Massimo Cenciarini and Aaron M Dollar. Biomechanical considerations in the design of lower limb exoskeletons. In *2011 IEEE International Conference on Rehabilitation Robotics*, pages 1–6. IEEE, 2011.

[9] Bing Chen, Hao Ma, Lai-Yin Qin, Fei Gao, Kai-Ming Chan, Sheung-Wai Law, Ling Qin, and Wei-Hsin Liao. Recent developments and challenges of lower extremity exoskeletons. *Journal of Orthopaedic Translation*, 5:26–37, 2016.

[10] Eugene Demaitre. The Robot Report. https://www.therobotreport.com/exoskeleton-developers-must-refine-capabilities-cost-says-maxon/, 2019.

[11] Grant Elliott, Andrew Marecki, and Hugh Herr. Design of a clutch–spring knee exoskeleton for running. *Journal of Medical Devices*, 8(3):031002, 2014.

[12] Ryan J Farris and Michael Goldfarb. Design of a multidisc electromechanical brake. *IEEE/ASME Transactions on mechatronics*, 16(6):985–993, 2010.

[13] Ryan J Farris, Hugo A Quintero, and Michael Goldfarb. Preliminary evaluation of a powered lower limb orthosis to aid walking in paraplegic individuals. *IEEE Transactions on Neural Systems and Rehabilitation Engineering*, 19(6):652–659, 2011.

[14] Ryan J Farris, Hugo A Quintero, Thomas J Withrow, and Michael Goldfarb. Design and simulation of a joint-coupled orthosis for regulating fes-aided gait. In *2009 IEEE International Conference on Robotics and Automation*, pages 1916–1922. IEEE, 2009.

[15] Michael Goldfarb and William K Durfee. Design of a controlled-brake orthosis for fes-aided gait. *IEEE Transactions on Rehabilitation Engineering*, 4(1):13–24, 1996.

[16] Hongtao Guo, Aaron See-Long Hung, Wei-Hsin Liao, Daniel Tik-Pui Fong, and Kai-Ming Chan. Gait analysis for designing a new assistive knee brace. In *2011 IEEE International Conference on Robotics and Biomimetics*, pages 1990–1995. IEEE, 2011.

[17] Hugh Herr. Exoskeletons and orthoses: classification, design challenges and future directions. *Journal of neuroengineering and rehabilitation*, 6(1):21, 2009.

[18] Joel Hruska. Extreme Tech , year = 1999, url = https://www.extremetech.com/extreme/222396-a-new-budget-exoskeleton-could-help-paraplegics-walk-at-a-drastically-lower-price/, urldate = 2010-09-30.

[19] Steven E Irby, Kenton R Kaufman, Roy W Wirta, and David H Sutherland. Optimization and application of a wrap-spring clutch to a dynamic knee-ankle-foot orthosis. *IEEE Transactions on Rehabilitation Engineering*, 7(2):130–134, 1999.

[20] Larry Jasinski. Rewalk Robotics. https://rewalk.com/restore-exo-suit/, 2011.

[21] Dr. George P. Johnson. Ankle ROM .

[22] F Jonsdottir, ET Thorarinsson, H Palsson, and KH Gudmundsson. Influence of parameter variations on the braking torque of a magnetorheological prosthetic knee. *Journal of intelligent material systems and structures*, 20(6):659–667, 2009.

[23] Rudi Kobetic, Curtis S To, John R Schnellenberger, Musa L Audu, Thomas C Bulea, Richard Gaudio, Gilles Pinault, Scott Tashman, and Ronald J Triolo. Development of hybrid orthosis for standing, walking, and stair climbing after

spinal cord injury. *Journal of Rehabilitation Research & Development*, 46(3), 2009.

[24] Madhero88. Lower Body Skeletal Muscles.

[25] Abhishek Rudra Pal and Dilip Kumar Pratihar. Estimation of joint torque and power consumption during sit-to-stand motion of human-being using a genetic algorithm. *Procedia Computer Science*, 96:1497–1506, 2016.

[26] Minerva Vasudevan Pillai. *Design of a Passive Dual Joint Stance Assistance Knee Exoskeleton*. PhD thesis, University of California, Berkeley, 2014.

[27] Carol Porth and Mary Pat Kunert. *Pathophysiology: Concepts of altered health states*, volume 781749883. Lippincott Williams & Wilkins Philadelphia, 2005.

[28] Jerry E Pratt, Benjamin T Krupp, Christopher J Morse, and Steven H Collins. The roboknee: an exoskeleton for enhancing strength and endurance during walking. In *IEEE International Conference on Robotics and Automation, 2004. Proceedings. ICRA'04. 2004*, volume 3, pages 2430–2435. IEEE, 2004.

[29] Elliott J Rouse, Luke M Mooney, Ernesto C Martinez-Villalpando, and Hugh M Herr. Clutchable series-elastic actuator: Design of a robotic knee prosthesis for minimum energy consumption. In *2013 IEEE 13th International Conference on Rehabilitation Robotics (ICORR)*, pages 1–6. IEEE, 2013.

[30] Arun Pal Singh. Knee Maximum ROM.

[31] Study.com. Online Website (Study.com).

[32] Tim Swift. Roam Robotics. https://www.roamrobotics.com/medical, 2013.

[33] Wayne Yi-Wei Tung. *Design and operation of minimally actuated medical exoskeletons for individuals with paralysis*. PhD thesis, UC Berkeley, 2013.

[34] Huseyin Atakan Varol, Frank Sup, and Michael Goldfarb. Powered sit-to-stand and assistive stand-to-sit framework for a powered transfemoral prosthesis. In *2009 IEEE International Conference on Rehabilitation Robotics*, pages 645–651. IEEE, 2009.

[35] Brian Weinberg, Jason Nikitczuk, Shyamal Patel, Benjamin Patritti, Constantinos Mavroidis, Paolo Bonato, and P Canavan. Design, control and human testing of an active knee rehabilitation orthotic device. In *Proceedings 2007 IEEE International Conference on Robotics and Automation*, pages 4126–4133. IEEE, 2007.

[36] Terris Yakimovich, Edward D Lemaire, and Jonathan Kofman. Engineering design review of stance-control knee-ankle-foot orthoses. *Journal of Rehabilitation Research & Development*, 46(2), 2009.

[37] yoshiyuki sankai. Cyberdyne HAL. https://www.cyberdyne.jp/english/products/fl05.html 2012.

[38] Karl E Zelik and Arthur D Kuo. Human walking isn't all hard work: evidence of soft tissue contributions to energy dissipation and return. *Journal of Experimental Biology*, 213(24):4257–4264, 2010.

Appendix A

SolidWorks Drawing

In this appendix the SolidWorks drawing files for the simple model are included.

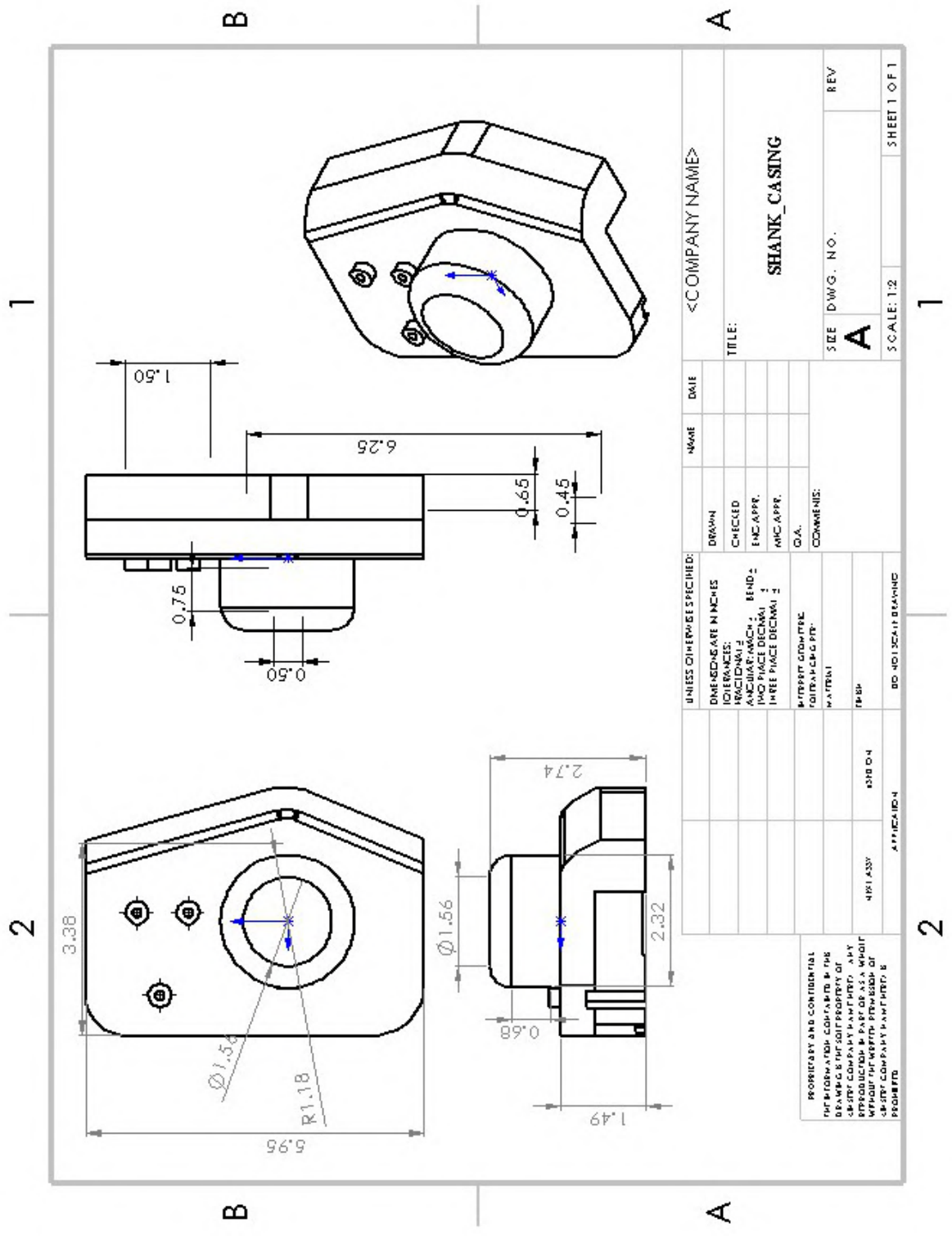

Figure A.1: Shank Casing

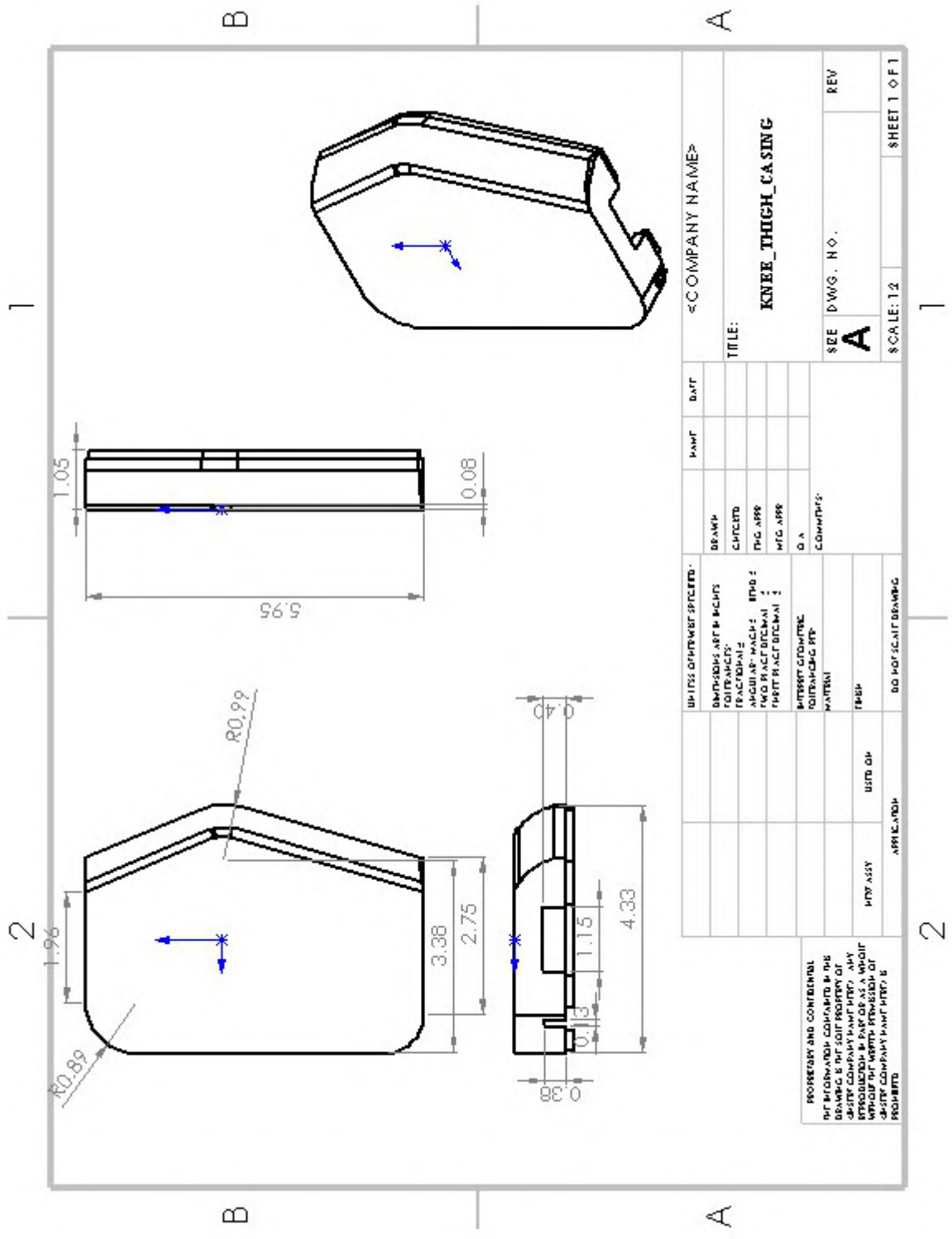

Figure A.2: Thigh Casing

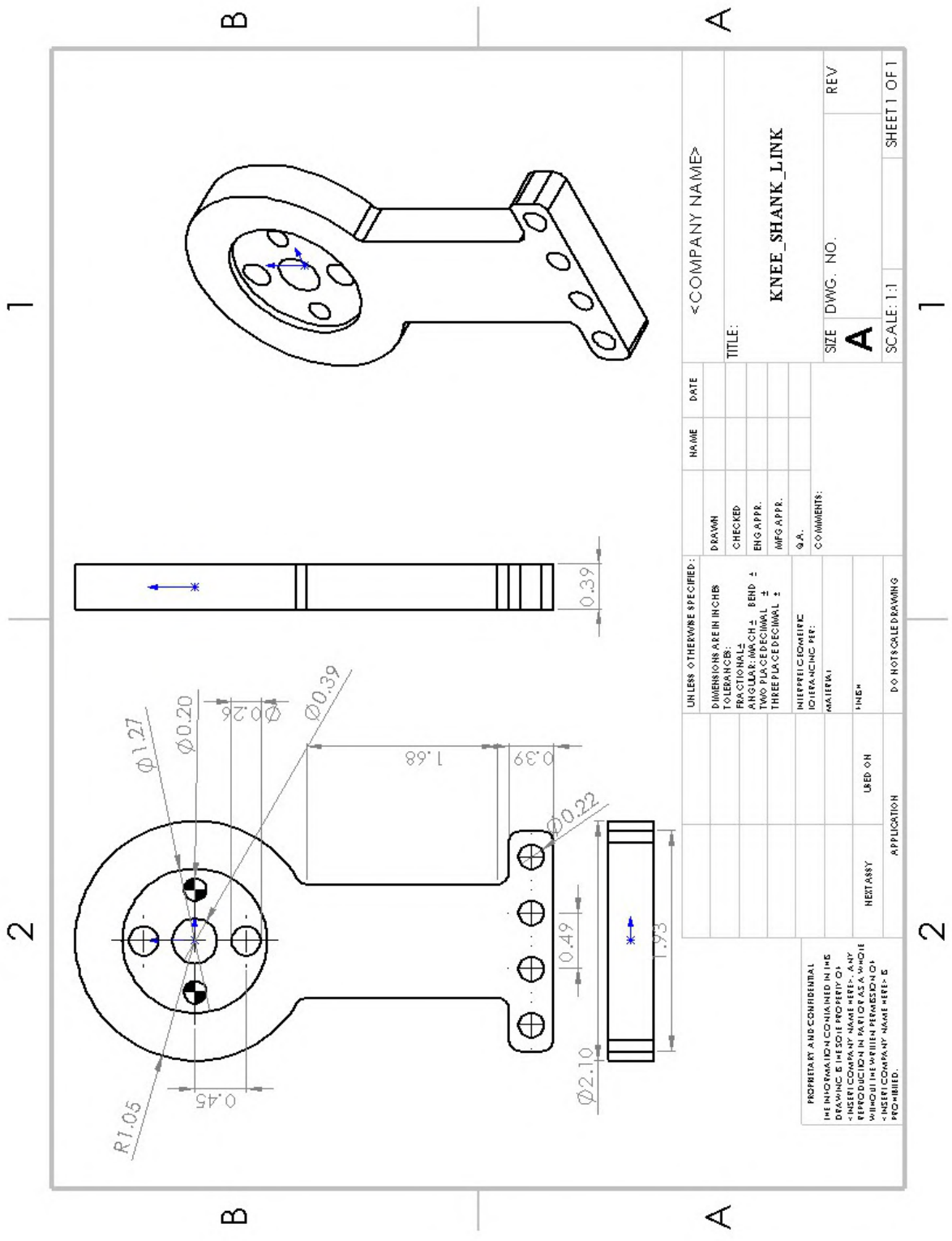

Figure A.3: Shank Link

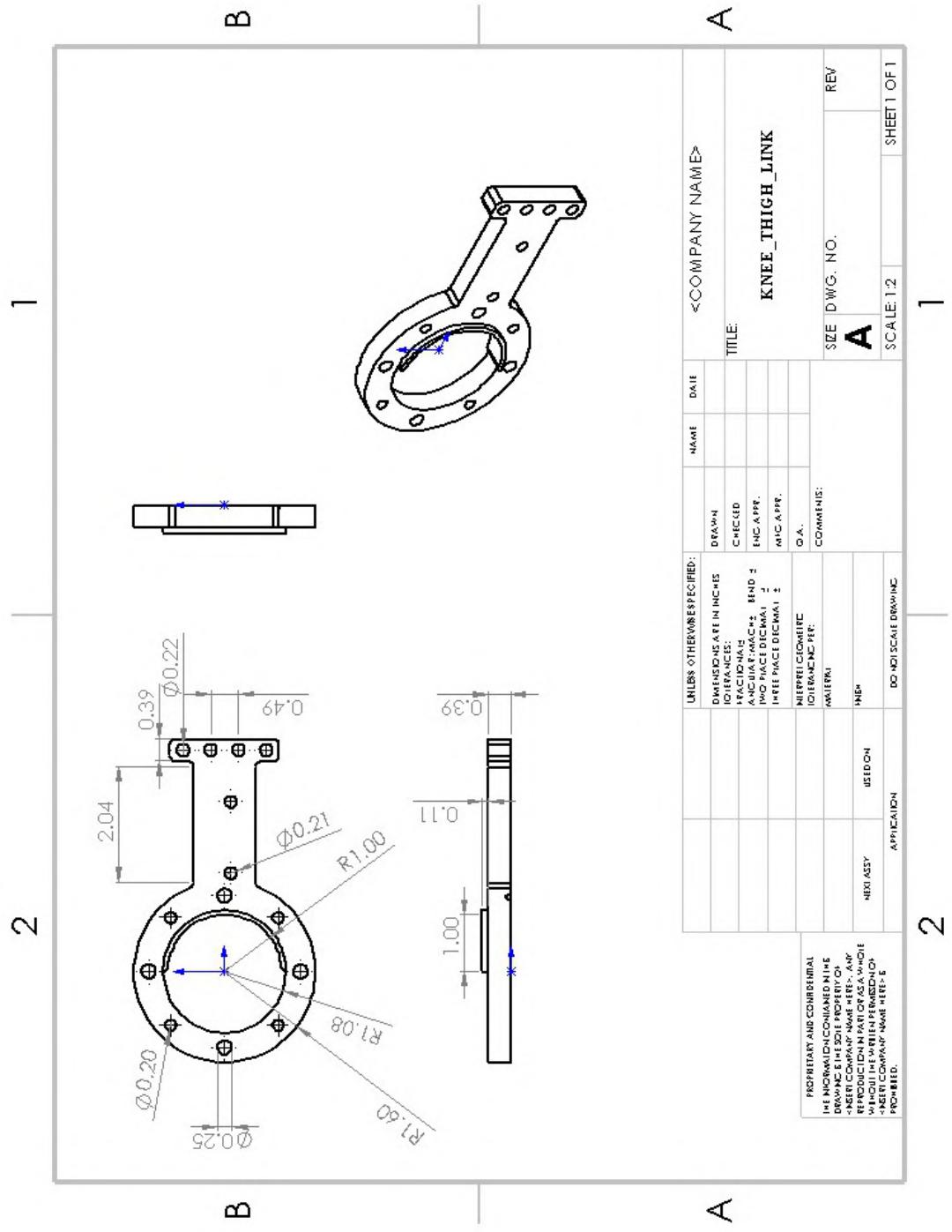

Figure A.4: Thigh Link

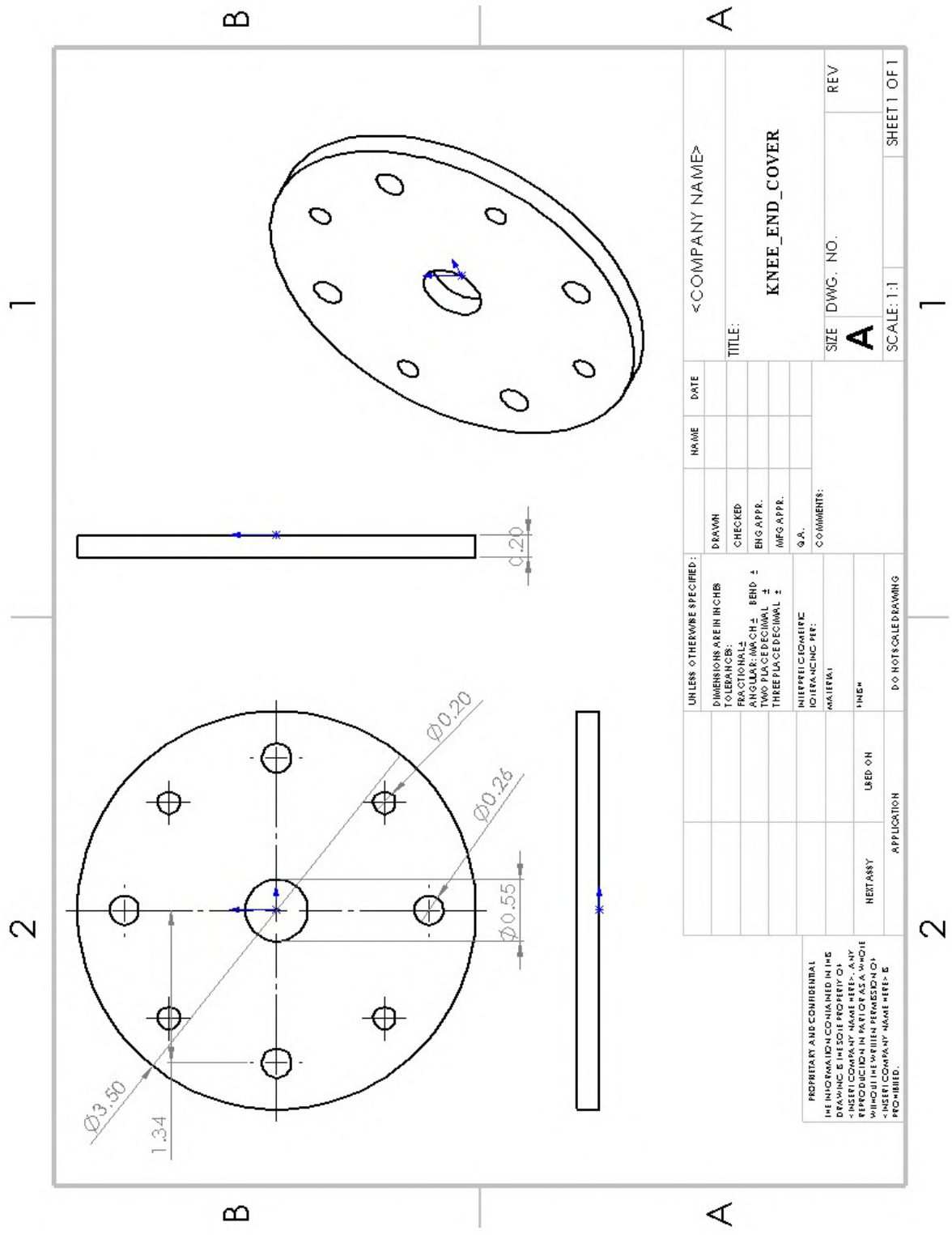

Figure A.5: Knee End Cover

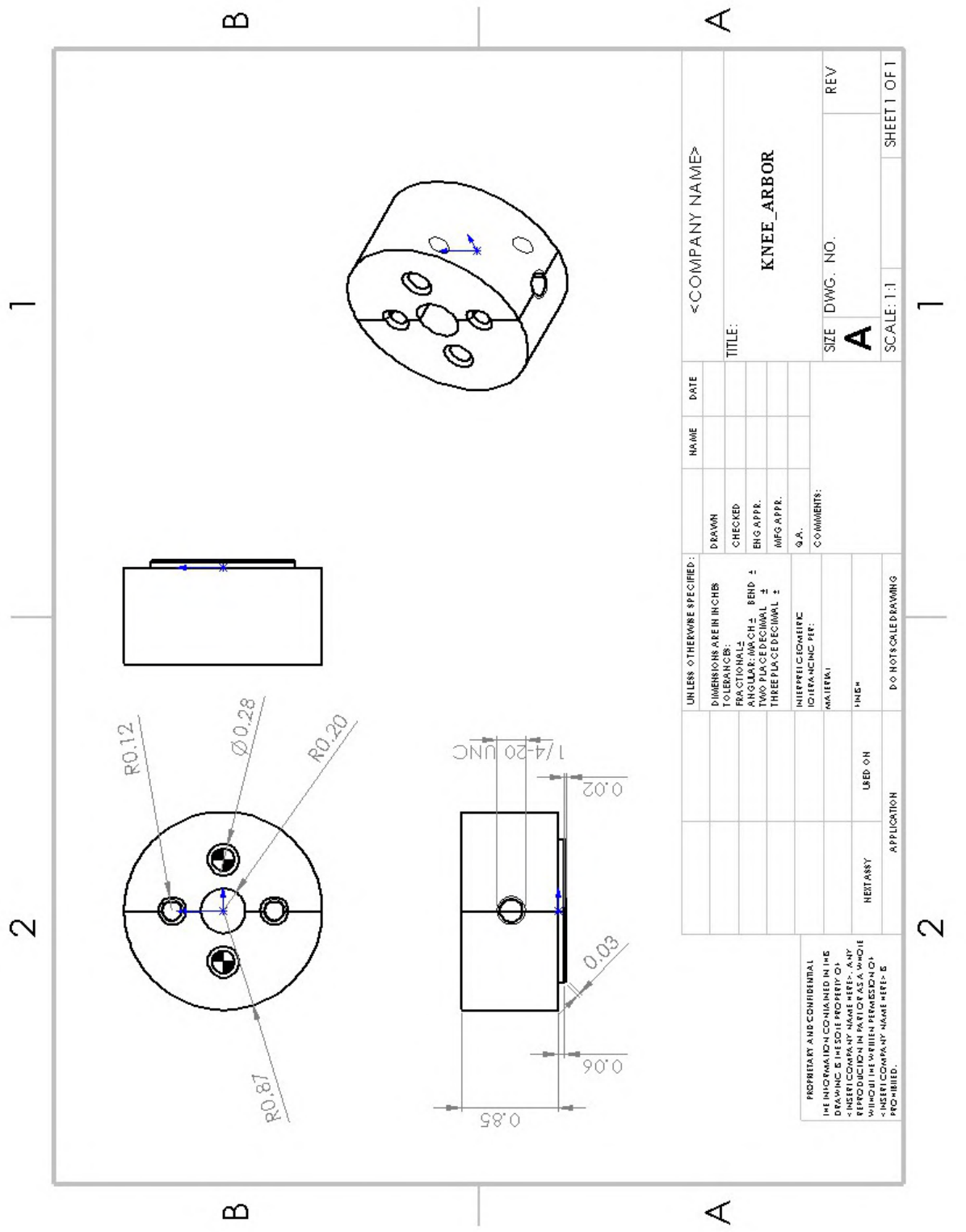

Figure A.6: Knee Arbor

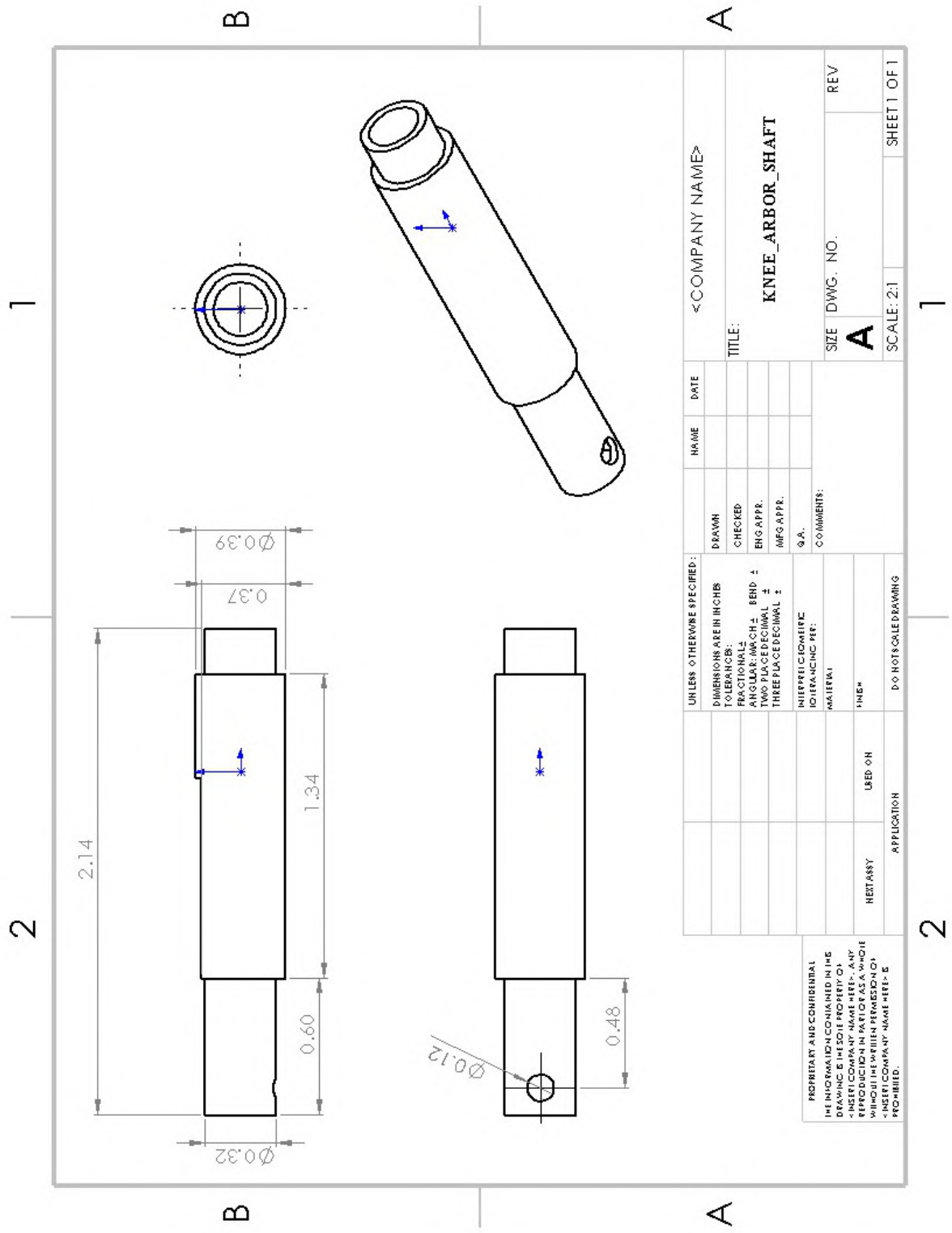

Figure A.7: Knee Arbor Shaft

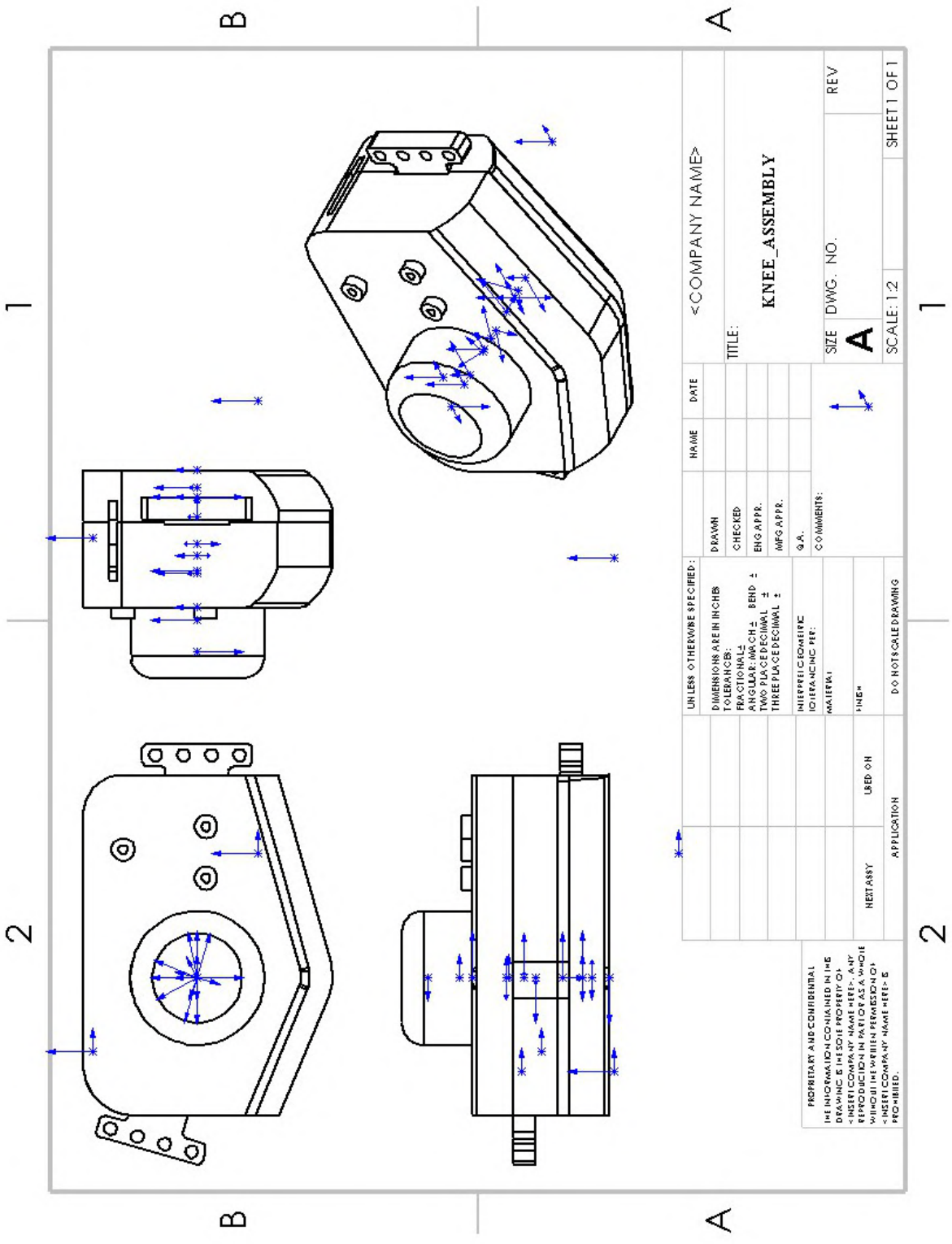

Figure A.8: Knee Assembly